NASA Technical Memorandum 107374

Predicted Turbine Heat Transfer for a Range of Test Conditions

R.J. Boyle and B.L. Lucci
Lewis Research Center
Cleveland, Ohio

Prepared for the
41st Gas Turbine and Aeroengine Congress
sponsored by the International Gas Turbine Institute of
the American Society of Mechanical Engineers
Birmingham, United Kingdom, June 10–13, 1996

National Aeronautics and
Space Administration

PREDICTED TURBINE HEAT TRANSFER FOR A RANGE OF TEST CONDITIONS

R. J. Boyle
NASA Lewis Research Center
Cleveland, OH 44135

B. L. Lucci
NASA Lewis Research Center
Cleveland, OH 44135

ABSTRACT

Comparisons are shown between predictions and experimental data for blade and endwall heat transfer. The comparisons are given for both vane and rotor geometries over an extensive range of Reynolds and Mach numbers. Comparisons are made with experimental data from a variety of sources. A number of turbulence models are available for predicting blade surface heat transfer, as well as aerodynamic performance. The results of an investigation to determine the turbulence model which gives the best agreement with experimental data over a wide range of test conditions are presented.

Nomenclature

c	-	True chord
c_x	-	Axial chord
c_p	-	Specific heat
d	-	Distance from surface
h	-	Span
Ec	-	Eckert number, $W_2^2/c_p/\|(T'_g - T_w)\|$
M_2	-	Isentropic exit relative Mach No.
Nu	-	Nusselt No. based on true chord and $k(T'_1)$
P	-	Pressure
Pr	-	Prandlt No.
Pr_t	-	Turbulent Prandlt No.
Re_2	-	Reynolds No. based on true chord and M_2
Sc	-	Schmidt number
St	-	Stanton number
St_m	-	Mass transfer Stanton number
s	-	Surface distance
T	-	Temperature
Tu	-	Turbulence intensity
W	-	Relative velocity
y_1^+	-	Normalized distance of first grid line from blade
δ	-	Inlet boundary layer thickness
μ_t	-	Turbulent eddy viscosity
ρ	-	Density

Subscripts

EXIT	-	Exit of computational domain
f	-	Full
$'$	-	Gas total condition
g	-	
w	-	Surface
1	-	inlet
2	-	outlet

INTRODUCTION

A relatively large number of three-dimensional Navier-Stokes analyses for turbine blade row heat transfer have been reported in the literature. Each of the reported results have shown comparisons with at most a few experimental cases. In order to validate an approach to predicting turbine blade row heat transfer, it is desirable to show comparisons with experimental data for an extended range of test conditions. Among the earliest heat transfer predictions using steady state three-dimensional analyses were those of Hah(1989) and Choi and Knight(1988). They showed comparisons with the experimental data of Graziani et al.(1980). The experimental data were for a large scale rotor geometry tested in a linear cascade at low Mach number. The tests were conducted with a uniform heat flux boundary condition which resulted in an average T_w/T'_g of approximately 1.08. Chima et al.(1993) showed comparisons of endwall heat transfer predictions with the experimental data of Boyle and Russell(1990). Again, the experimental data were for a large scale, relatively low speed linear cascade, with low turbulence intensity and a $T_w/T'_g = 1.07$. Data have been obtained on a large scale rotating turbine rotor by Blair(1994). These data were for a variety of Reynolds numbers and incidence angles. In these tests the Mach numbers were relatively low, and the average $T_w/T'_g = 1.1$. Data for stator vanes at transonic Mach numbers and wall-to-gas temperature ratios typical of gas turbine applications have been measured by a number of researchers. York et al.(1984) obtained data in a linear cascade for a

Table I. - Description of cases used in analysis

Vanes					
Source of data	$Re_{2c}X10^{-5}$	M_{EXIT}	T_w/T_g'	Cascade	Test approach
York et al.(1984)	2.1-18.0	0.3-1.1	0.75	Linear	Steady state
Arts and Heider(1994)	22.5	0.92-1.15	0.73	Annular	Shock tube
Boyle and Russell(1990)	3.4-20	0.1-0.7	1.1	Linear	Liquid Crystals
Harasagama and Wedlake(1990)	17-52	0.94-1.29	0.66	Annular	Shock tube
Rotors					
Source of data	$Re_{2c}X10^{-5}$	M_{EXIT}	T_w/T_g'	Cascade	Test approach
Blair(1994)	2.7-7.1	0.06-0.15	1.1	Rotating	Steady state
Goldstein and Spores(1988)	1.4-2.3	0.03-0.04	1	Linear	Napthalene
Chen and Goldstein(1992)	1.2-2.0	0.02-0.03	1	Linear	Napthalene
Graziani et al.(1980)	10.7	0.1	1.1	Linear	Steady state
Giel et al.(1996)	13-26	1.0-1.3	1.1	Linear	Steady state

Table II. - Characteristics of experimental data

Vanes						
Source of data	$Tu\%$	Heat Transfer		$(T_w)_1/T_g'$	Ec	No. of
		Endwall	Blade			Cases
York et al.(1984)	7.0	Y	N	1.0	1.56	4
Arts and Heider(1994)	4.5	Y	Y	0.73	1.56	1
Boyle and Russell(1990)	1.0	Y	N	1.0	1.51	2
Harasagama and Wedlake(1990)	6.5	Y	Y	0.66	1.47	5
Rotors						
Source of data	$Tu\%$	Heat Transfer		$(T_w)_1/T_g'$	Ec	No. of
		Endwall	Blade			Cases
Blair(1994)	High	Y	Y	1.0	0.15	3
Goldstein and Spores(1988)	1.2	Y	N	1.0	N.A.	3
Chen and Goldstein(1992)	1.2	N	Y	1.0	N.A.	1
Graziani et al.(1980)	1	Y	Y	1.0	0.18	2
Giel et al.(1995)	0.3-7	Y	N	1.0	5.3-8	4

stator vane configuration. Harasagama and Wedlake(1991), Chana(1992), and Arts and Heider(1994) presented stator vane heat transfer obtained in shock tube facilities for annular cascades. Predictions using three-dimensional Navier-Stokes analyses were obtained by Heider and Arts(1994) for the data of Arts and Heider(1994), and by Boyle and Jackson(1995) for the data of Chana(1994).

In general most predictions presented in the literature showed comparisons with a limited number of experimental cases. The data available in the literature cover a wide variety of test conditions. In addition to a range of geometries, Reynolds and Mach numbers, there are significant differences in turbulence intensity, inlet boundary layer thicknesses, as well as inlet blade row temperature profile among the experimental data.

The work reported herein consists of comparisons of predicted blade row heat transfer with experimental data for a variety of test configurations. The purpose of examining a variety of test configurations is to increase confidence in the ability of both the analysis and turbulence model to predict blade row heat transfer. The analysis was done using the steady state three-dimensional Navier-Stokes code described by Chima(1991), and by Chima and Yokota(1988). Results were obtained using algebraic turbulence models.

EXPERIMENTAL DATA USED FOR VERIFICATION

Table I gives a description of the experimental data sources with which the computational results are compared. There are four stator and four rotor geometries. The data of Goldstein and Spores(1988) are for the same rotor geometry as Chen and Goldstein(1992). The maximum Mach number for each of the stator tests is in the transonic flow regime, but only the rotor test data of Giel et al.(1996) is in the transonic region. Except for the data of Graziani et al.(1980), the

Table III. - Characteristics of cases examined

Vanes									
Source of data	c_x,(cm)	c_t/c_x	h/c_x	δ_f/c_x	Re_2X10^{-5}	Re_1/Re_2	P_2/P_1'	y_1/c_x	$(T_w)_1/T_g'$
York et al.(1984)	5.25	1.775	1.45	0.12	2.1	0.36	0.951	2.8e-05	1.0
				0.12	6.2	0.32	0.721	2.2e-05	1.0
				0.12	18.0	0.32	0.721	8.0e-06	1.0
				0.12	18.0	0.30	0.468	7.4e-06	1.0
Arts and Heider(1994)	4.21	1.836	1.19	0.0012	22.5	0.25	0.440	1.0e-05	0.73
Boyle and Russell(1990)	13.8	1.393	1.104	0.184	3.4	0.35	0.996	0.9e-04	1.0
				0.184	20.0	0.35	0.836	1.8e-05	1.0
Harasagama and Wedlake(1990)	3.96	1.881	1.26	0.093	34.0	0.25	0.566	5.6e-06	0.659
					34.0	0.24	0.445	5.0e-06	0.659
					34.0	0.23	0.366	4.7e-06	0.659
					17.0	0.24	0.445	9.4e-06	0.659
					52.0	0.24	0.445	3.4e-06	0.659

Rotors									
Source of data	c_x,(cm)	c_t/c_x	h/c_x	δ_f/c_x	Re_2X10^{-5}	Re_1/Re_2	P_{EXIT}	y_1/c_x	$(T_w)_1/T_g'$
Blair(1994)	16.1	1.22	0.946	0.05	2.7	0.59	0.997	1.0e-04	1.0
				0.05	2.7	0.78	0.997	1.0e-04	1.0
				0.05	7.1	0.78	0.980	1.0e-04	1.0
Goldstein and Spores(1988)	14.53	1.1641	2.065	0.10	2.3	0.61	0.998	1.0e-04	1
				0.20	2.3	0.61	0.998	1.0e-04	1
				0.08	1.4	0.61	0.999	1.5e-04	1
Chen and Goldstein(1992)	14.53	1.1641	2.065	0.18	2.0	0.61	0.998	1.0e-04	1
Graziani et al.(1980)	28.13	1.22	0.99	0.014	10.8	0.63	0.985	3.0e-05	1.0
				0.117	10.8	0.63	0.985	3.0e-05	1.0
Giel et al.(1996)	12.7	1.45	1.20	0.24	26.	0.53	0.361	7.4e-06	1.00
				0.27	13.	0.53	0.361	1.4e-05	1.00
				0.15	26.	0.53	0.361	7.4e-06	1.00
				0.24	26.	0.53	0.528	8.9e-06	1.00

low Mach numbers are associated with low Reynolds numbers. Except for the data of Boyle and Russell(1990), the stator data are all for T_w/T_g' values representative of actual engine applications. The data for rotor geometries are all for T_w/T_g' close to unity. Data obtained using liquid crystals or Napthalene permit near continuous measurement of the surface heat transfer. Blair(1994) obtained data in a rotating large scale facility for a range of incidences.

Table II gives characteristics of the various data sources. The data of Boyle and Russell(1990) were for a low turbulence intensity, while the other stator data were for moderate to high levels of turbulence. All cases had endwall data, and Arts and Heider(1994) and Harasagama and Wedlake(1990) showed vane heat transfer data. High turbulence levels were present in Blair's test and for some of the tests of Giel et al. The other rotor data had low turbulence levels.

Table II also lists the Eckert,Ec, numbers for each data source. The values shown are for the maximum blade row exit velocity for each data set. The Ec number indicates the importance of viscous dissipation in determining the near wall temperature profile. All of the stator test cases have maximum Ec numbers greater than one, while only the rotor cases of Giel et al. had Ec values greater than 0.2. Because the cases with wall-to-gas temperature ratios representative of actual engine conditions also have high exit Mach numbers, these cases also have relatively high Eckert numbers.

Table III shows geometric, flow, and thermal characteristics of the various cases examined. The inlet and exit Reynolds numbers are shown for each test case. Both Reynolds numbers are given to facilitate comparisons among different investigators. Some experimental heat transfer results were given using inlet conditions, while others used exit conditions. Those cases where the inlet wall temperature ratio,$(T_w)_1/T_g'$, is given as unity have unheated,(or uncooled in the case of York et al.), starting lengths. This table also shows the near wall spacing used in the computational analysis. This is the spacing of the first grid line from either the blade or endwall surface. This spacing, y_1/c_x, was determined from a flat plate correlation so as to give a y_1^+ of approximately one.

DESCRIPTION OF COMPUTATIONAL ANALYSIS

Steady state heat transfer predictions were made using the three-dimensional Navier-Stokes computer code RVC3D. This code is a finite difference analysis, and was described by Chima(1991), and by Chima and Yokota(1988). The analysis used a Runge-Kutta time marching approach. Implicit residual smoothing is used to improve convergence. Three algebraic turbulence models are available for use in the code. These models can be viewed as variations of the commonly used Baldwin-Lomax(1978) algebraic turbulence model. Cases were run using each of the three turbulence models. Results are presented herein for the turbulence model which gave the best agreement with experimental data overall. The model chosen is the one described by Chima et al.(1993). Predictions using an alternative turbulence model are given for selected cases.

Since many of these test cases, and actual engine operation, were at relatively high turbulence levels, the transition criteria of Mayle(1991) was incorporated into the turbulence model. The Baldwin-Lomax transition criteria does not account for freestream turbulence effects. High freestream turbulence results in leading edge Frossling numbers significantly greater than unity. To account for the effect of freestream turbulence on laminar heat transfer, the model of Smith and Kuethe(1966) was incorporated into the calculation of turbulent viscosity.

Researchers showed good agreement between predicted and measured turbine blade heat transfer using both algebraic and two-equation turbulence models. For example, the experimental cascade data of Graziani et al.(1980) have been used for a number of different heat transfer predictions. Hah(1989), and Choi and Knight(1988) used two-equations turbulence models to predict the blade and endwall heat transfer. Ameri and Arnone(1994) analyzed this case using both two-equation and algebraic turbulence models. All of the predictions agree reasonably well with the experimental data. The aforementioned experimental case, along with several other available in the literature, is for low Mach number flow. It remains to be seen if algebraic models are as effective as two equation models in predicting turbine blade heat transfer for high Mach and Reynolds number cases. As shown by Ameri and Arnone(1994), heat transfer predictions using two-equation models required nearly twice the CPU time to converge, compared with an algebraic model solution. Results are presented herein for high Reynolds number cases, which require a moderate to large number of grid points. Since two equation turbulence models have not demonstrated a significant superiority over algebraic models for turbine blade heat transfer predictions, and CPU time is a significant consideration, algebraic turbulence models were used. Both Pr and Pr_t were held constant at 0.70 and 0.90 respectively.

A uniform temperature boundary condition was imposed on all solid boundaries. Spanwise radial equilibrium was assumed at the exit boundary. At each spanwise location the exit static pressure was allowed to vary in the circumferential direction. The average hub exit static pressure was specified, but the pitchwise variation was determined from the internal flow field. Uniform total conditions were specified for the inlet core flow, and uniform static pressures were specified through the boundary layers. The inlet boundary layer temperature and velocity profiles were determined using flat plate correlations in which the friction factor and Stanton number are determined by the specified inlet boundary layer thickness. The correlations are those given by Kays and Crawford(1980). Using a simple power law for the inlet temperature profile produces an erroneous result, since the power law gives an infinite gradient at the wall.

A large number of cases were examined, placing a premium on obtaing solutions with a minimum of CPU time. Therefore, moderate size grids were used. A typical grid size was $185 \times 49 \times 65$, and was chosen based on previous work, (Boyle and Giel(1992)). Even though midspan symmetry was assumed for the linear geometry test cases, 65 spanwise grid lines were used to maintain a desirable stretching ratio for the high Reynolds number test cases. C-type grids were generated using the procedure described by Arnone et. al.(1992). In this procedure grid lines near the surfaces are embedded within a coarse grid, which is generated using Sorenson's(1980) technique. It was found necessary to maintain grid stretching ratios less than 1.3 in addition to having a y_1^+ near unity to obtain grid independent results.

The primary convergence criteria was that the surface heat transfer remained constant as the solution advanced in time. It was observed that the ratio of inlet to exit mass flow varied greatly during the first five hundred or so iterations. In addition to the stability in the surface heat transfer, cases were run until there was only a small variation between the inlet and exit mass flow. When these criteria were met, it was found that the residuals had decreased by three or more orders of magnitude. The analysis was run on a Cray C90 machine. The CPU time for convergence was between one and three hours, with the low Mach number cases requiring the most time. The low Mach number cases were run with a minimum P_2/P_1' of 0.985 and the experimental Reynolds number to improve convergence speed. A test case with a higher pressure ratio, and the same Reynolds number took significantly longer to converge to the same result. The computer code was vectorized by the developer, Chima(1991). Consequently, the average CPU time per grid point to advance the solution one time cycle was 6×10^{-6} seconds.

DISCUSSION of RESULTS

Table II shows that 25 cases were examined. Only selected cases will be compared graphically, although the predictions for all cases will be discussed.

Vanes

Comparison with data of York et al.(1984) The data of York et al.(1984) were for a range of test conditions, but results were presented for only a single representative case. The report by Hylton et al.(1981) contained the data for the test matrix. Heat transfer coefficients were presented in terms of Stanton number based on local conditions. Figure 1 shows comparisons between the predicted and measured Stanton numbers for the $M_2 = 0.27$ and $Re_2 = 2.1 \times 10^5$ case, and the $M_2 = 1.1$, and $Re_2 = 18. \times 10^5$ case. The Stanton number based on inlet conditions is also given for the higher Mach number case. It is included to facilitate comparisons with data from other sources. In this plot a percentage variation in Stanton number represents the same percentage variation in heat transfer coefficient.

The predictions, and to some extent the experimental data, show very high values close to the leading edge of the pressure surface. This is a result of the Stanton number definition used. These high Stanton numbers do not represent regions of high heat transfer coefficients, since this is a low velocity region. With this definition, when the velocity decreases, the Stanton number increases, even when the heat transfer coefficient is constant. The average predicted Stanton number agrees well with the average experimental Stanton number. Comparing the Stanton number based on local velocity predictions with experimental values shows some differences in the endwall heat transfer patterns. Part of the differences in heat transfer patterns could be due to differences in the choice of ΔT used to determine the Stanton number. In the predictions the endwall pressure distribution was used to determine the local velocity for the Stanton number, as well as the adiabatic wall temperature. The reference ΔT in the experimental Stanton number was based on an experimentally determined adiabatic wall temperature. The experimental adiabatic wall temperatures were considerably lower than adiabatic wall temperatures calculated assuming a recovery factor of $Pr^{0.333}$. Using the experimentl adiabatic wall temperature to determine the predicted Stanton numbers, increases the values by up to 30%.

The third plot for the higher Mach number case shows Stanton number based on inlet velocity. Here the heat transfer coefficient and Stanton number are proportional. The maximum heat transfer occurs in the midpassage upstream of the throat. In the unguided portion of the passage there is a decrease in heat transfer across the passage in moving from the pressure side to the suction surface. This same pattern was observed by Georgiou et al.(1979) in tests of a stator vane, conducted in a shock tube facility.

Upstream of the vane the predictions show a noticeable degree of pitchwise nonuniformity. This is partially due to the interaction of the unheated starting length boundary condition with a C-type grid. C-type grids have nonuniform spacing near the mid-pitch line at the inlet, which results in pitchwise non-uniform Stanton number contours near the endwall temperature discontinuity. However, as will be shown subsequently, C-type grids have an advantage in predicting the Stanton number in the leading edge region for the endwall and blade. Also, the Stanton number nonuniformity occurs only when there is a step change in endwall temperatures near the inlet. Calculations in which the location of the start of endwall cooling was varied, or with different grid spacing in the region on the temperature discontinuity, showed virtually identical heat transfer within the blade passage.

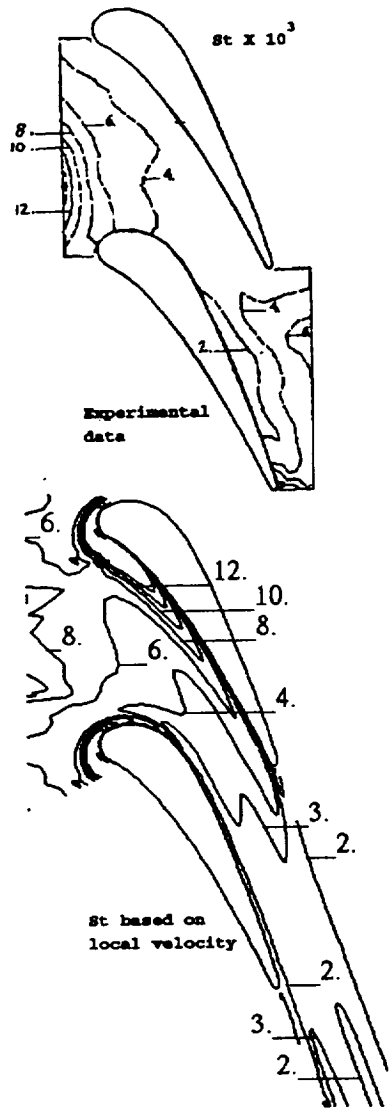

Fig. 1a - Comparison of endwall Stanton No. Data of York et al., $Re_2 = 2.1 \times 10^5, M_2 = 0.27$

Although not shown in the figure, comparisons for two $M_2 = 0.70$ cases at different Reynolds numbers were very similar to the comparisons for the $M_2 = 1.1$ case shown. Considering the results for all cases, the degree of agreement between the analysis and the data is reasonably good.

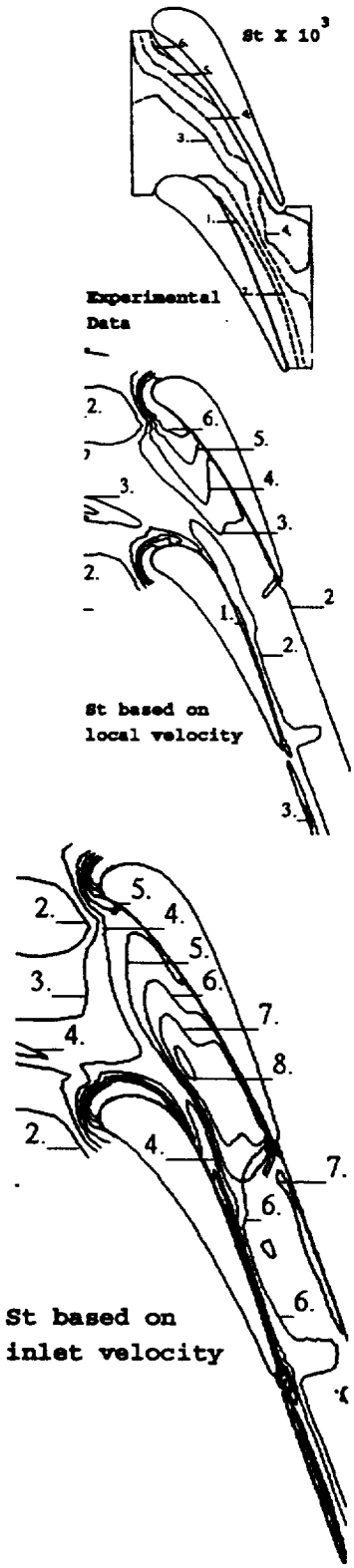

Fig. 1b - Comparison of endwall Stanton No. Data of York et al., $Re_2 = 18. \times 10^5$, $M_2 = 1.1$

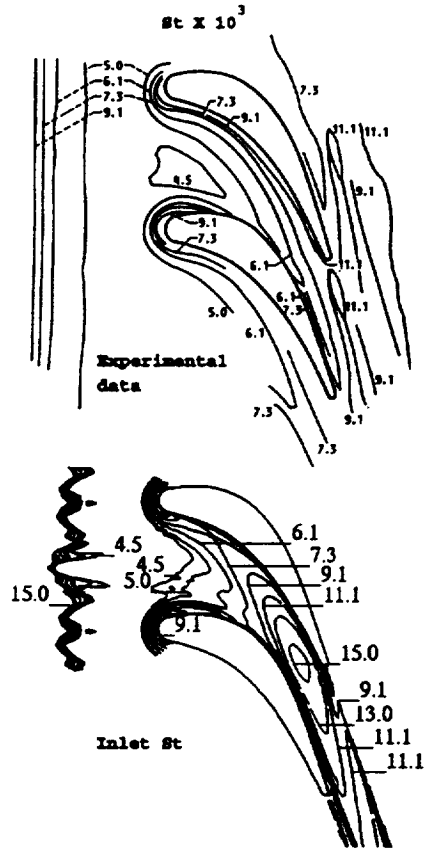

Fig. 2a - Comparison of endwall Stanton No. Data of Boyle and Russell, $Re_2 = 3.4 \times 10^5$

Data of Boyle and Russell. In these tests the Reynolds number was varied by varying the speed of the air through the cascade. Consequently, there was no independent variation of Reynolds and Mach numbers. In addition to varying the Reynolds number, the effects of variation of inlet boundary layer thickness were also presented by Boyle and Russell. The effects of variation in inlet boundary layer thickness were small. Comparisons are shown in figure 2 for a single inlet boundary layer thickness at the highest and lowest Reynolds numbers tested. Parts a and b of figure 2 compare predicted and measured Stanton numbers based on inlet conditions for two Reynolds numbers.

Within the passage the analysis overpredicts the Stanton number to a considerable extent. The region within the passage which shows the greatest disagreement is near the throat. For the low Reynolds number case the predictions show only a very small region near the pressure side of the throat with a Stanton number of 11.1×10^{-3}. But, the predictions show a peak level in excess of 15×10^{-3} in the same region. Close to the leading edge region the analysis is better agreement with the data. The liquid crystal measurements show a series of heat transfer contours in front of the leading

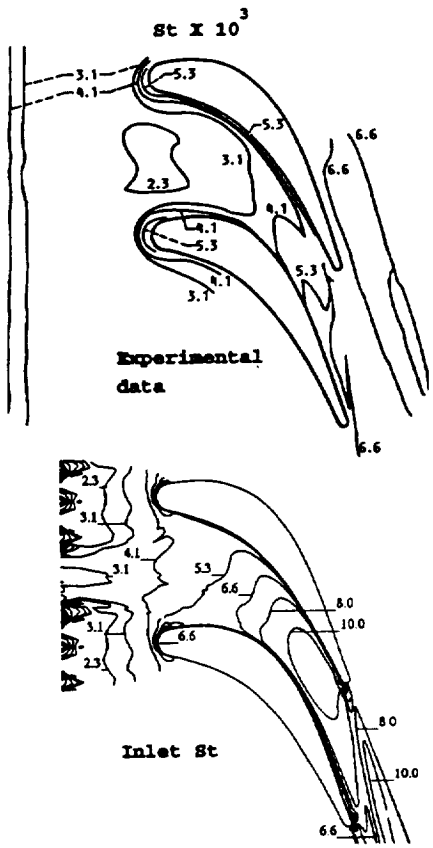

Fig. 2b - Comparison of endwall Stanton No. Data of Boyle and Russell, $Re_2 = 20 \times 10^5$

edge. The heat transfer rates increase substantially in approaching the leading edge. Boyle and Russell showed leading edge augmentation approaching a factor of three at 0.2× the leading edge diameter in front of the leading edge. The predictions show a series of nearly concentric contours, which agree well with the measurements in terms of location and level of augmentation.

For the high Reynolds number case the analysis overpredicts the heat transfer in the throat region. As will be shown, a significant amount of overprediction was due to the choice of turbulence model. To insure that the discrepancy in the heat transfer prediction was due to the choice of turbulence model, other factors were examined computationally. The vane was neither heated nor cooled, and the endwall was subjected to a nearly constant heat flux. There was no significant difference in the calculated endwall heat transfer when the vane was unheated compared to when it was maintained at the endwall temperature. There was also no significant variation in endwall Stanton number when the endwall was subject to a uniform heat flux boundary condition.

Data of Arts and Heider. Figure 3 shows a comparison of the predicted and measured heat transfer data of Arts and Heider(1994). These data were obtained in a shock tube so that uncertainties due to a step change in the endwall thermal boundary condition do not arise. The data are for

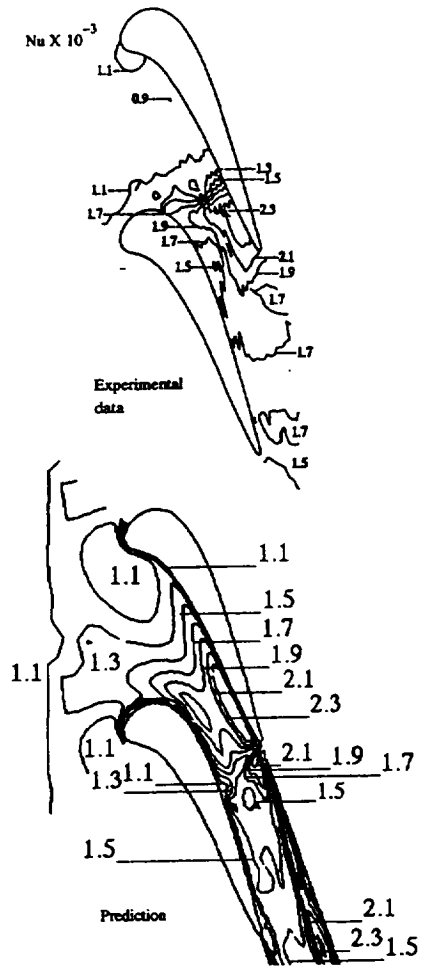

Fig. 3a- Comparison of hub Nusselt No. Data of Arts and Heider.

a stator at transonic exit conditions. The data were given as heat transfer coefficients, and have been normalized by the true chord and inlet conductivity to yield Nusselt numbers. There is good agreement between the predicted and measured Nusselt numbers for both the hub and casing surfaces.

In the experiment vane surface heat transfer measurements were made at 6%, 50%, and 94% of span. Figure 3c compares the measured and predicted heat transfer for the vane. For the pressure surface the measurements and predictions show little spanwise variation in heat transfer, though the analysis is somewhat greater than the data. Because of the high Reynolds number and moderate turbulence intensity, the predictions for the pressure surface gave transition close to the leading edge. The degree of agreement was significantly affected by the choice of transition length model. In the transition model the local turbulence intensity was adjusted based on the local freestream velocity. The analysis predicts the heat transfer well close to the endwall. At the midspan after transition, in what is essentially the uncovered portion of the vane, the analysis overpredicts the suction surface heat transfer. It will be shown that this overprediction is largely do to the choice of turbulence model.

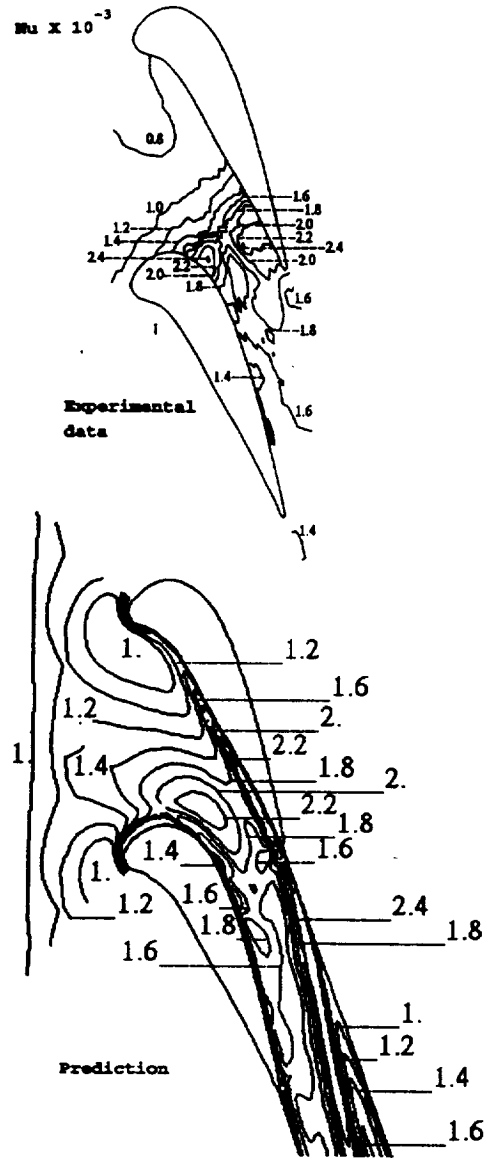

Fig. 3b Tip Nusselt No. Data of Arts and Heider.

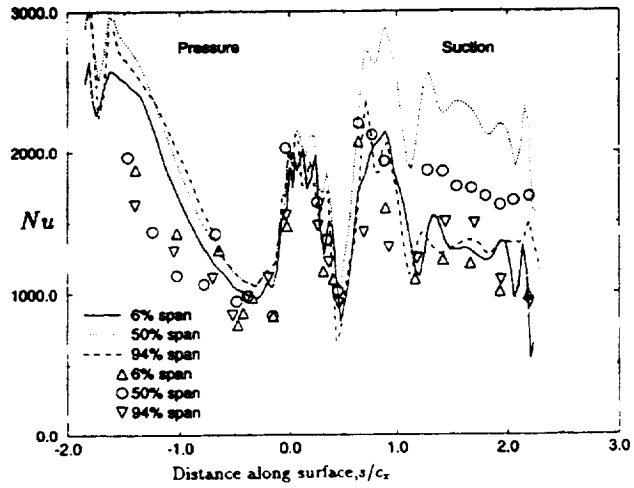

Fig. 3c Vane surface Nusselt No. Data of Arts and Heider.

Data of Harasagama and Wedlake. Figure 4 compares hub and vane heat transfer results for two different Reynolds numbers. This case is for a $M_2 = 1.14$. Vane heat transfer is mainly affected by variations in Reynolds number.

The Nusselt number varies with Reynolds number, but the degree of agreement between the prediction and measurement remains about the same. The analysis predicts a small, higher than measured, heat transfer region close to the pressure surface. Also, near the suction surface the analysis predicts a region of too low heat transfer aft of the throat region. The analysis overpredicts suction surface heat transfer in the transition region, and is slightly higher for the uncovered portion of the vane. While the variation in Nusselt number is not large, both the prediction and measurements show a lower heat transfer close to the suction surface downstream of the throat as the Mach number increases.

The degree of agreement between the analysis and the data for the casing heat transfer was about the same as for the hub. Variations in exit Mach number did not significantly affect the degree of agreement with the experimental data. The degree of agreement for the vane surface heat transfer was also not affected by variations in Mach number.

Rotors

Data of Graziani et al. Figure 5 compares the predictions with the measurements of Graziani et al. for the thin inlet boundary layer thicknesses. The measurements for the rotor surface show a slightly larger spanwise region of two-dimensional heat transfer distribution for the thinner boundary layer. In general the analysis overpredicts the heat transfer on both the rotor blade and endwall. On the rotor the analysis overpredicts the heat transfer on the rear portion of the pressure surface. This is a consequence of the transition model used. The model gave a good prediction for the suction surface transition location for the vane data of Arts and Heider. However, for this rotor case, the model predicted transition close to the leading edge. An adverse pressure gradient, close to the leading edge resulted in a calculated Re_θ sufficient to trigger transition in the turbulence model. Evidently, pressure surface transition did not occur in the experiment. On the suction surface the Stanton number is too high at transition, but otherwise the analysis predicts the heat transfer distribution reasonably well. The analysis severely overpredicts the endwall heat transfer. The largest overprediction occurs near the throat region. The effects of using a different turbulence model will be examined subsequently for this case.

Neither the measurements nor the predictions showed a large effect of varying the inlet boundary layer thickness on either the rotor blade or the endwall heat transfer. Both showed a slight decrease in peak passage heat transfer for the thicker inlet boundary layer.

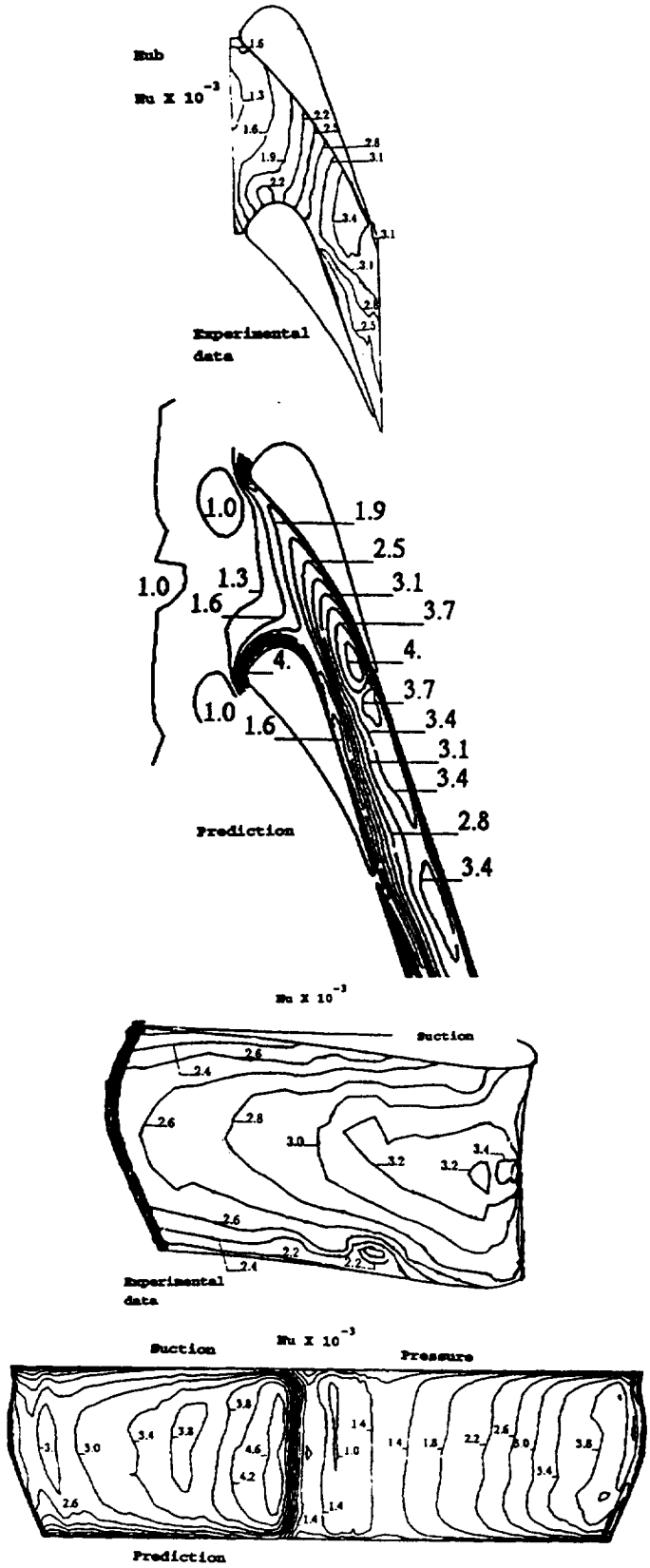

Fig. 4a- Nusselt No. comparisons. Data of Harasagama and Wedlake, $Re_2 = 34 \times 10^5, M_2 = 1.14$

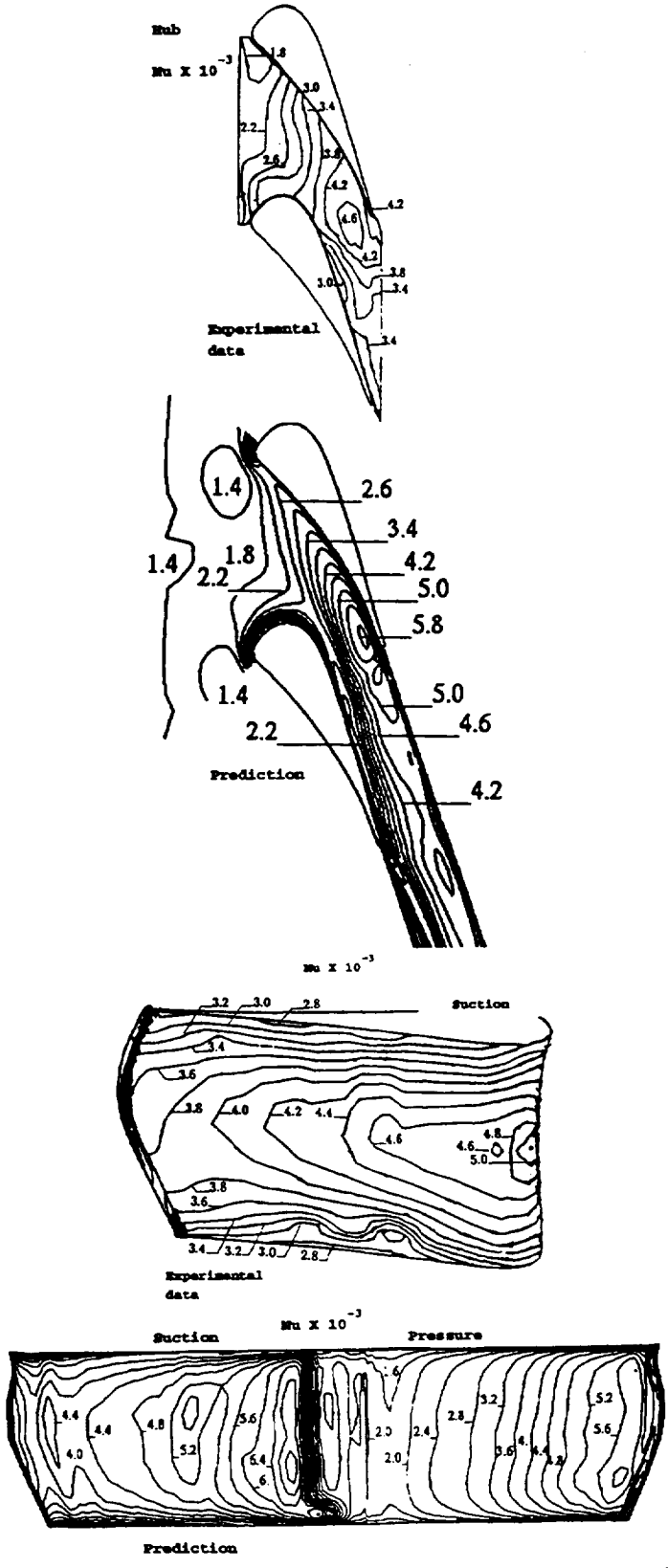

Fig. 4b- Nusselt No. comparisons. Data of Harasagama and Wedlake, $Re_2 = 54 \times 10^5, M_2 = 1.14$

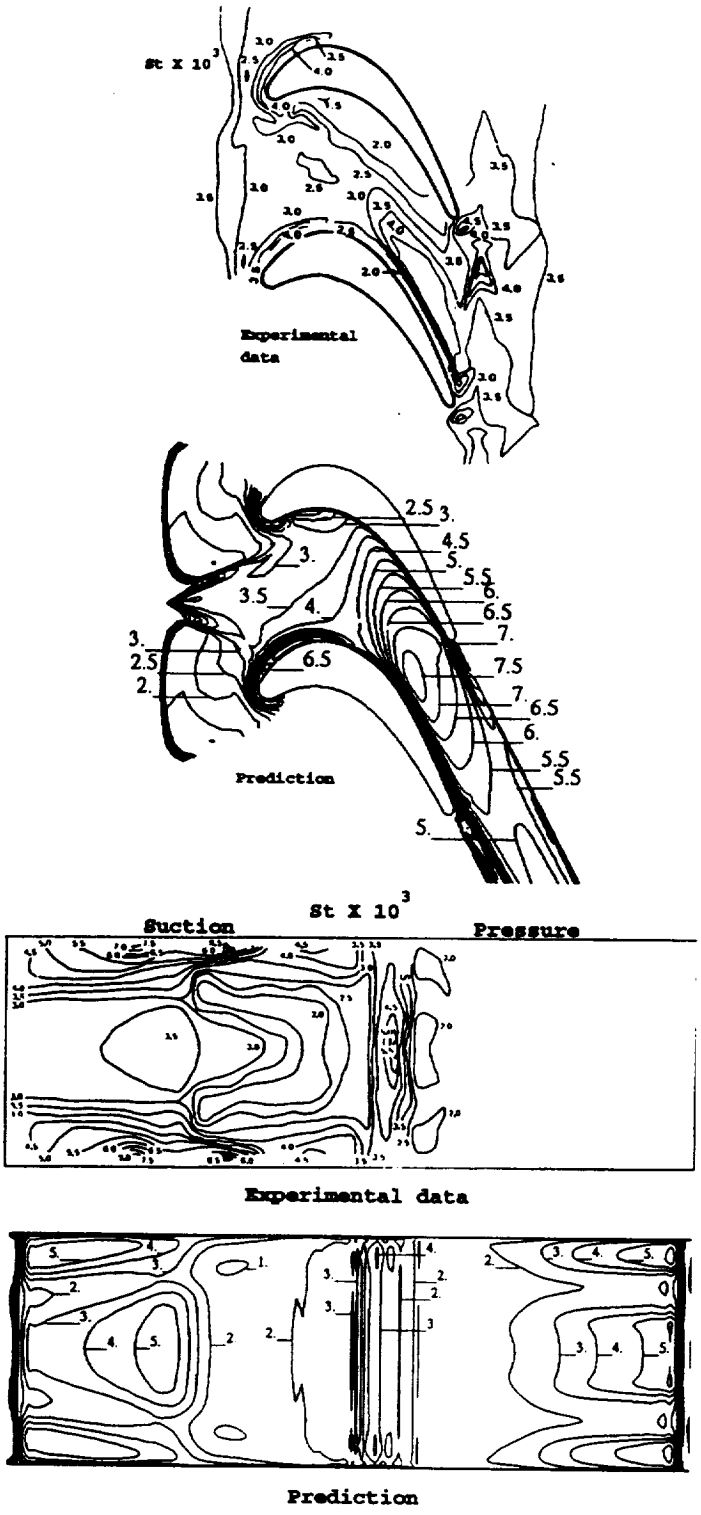

Fig. 5- Stanton No. comparisons. Data of Graziani et al.; thin inlet boundary layer.

Data of Goldstein and Spores. Figure 6a compares the predicted and measured endwall heat transfer for the higher Reynolds number-thin inlet boundary layer case of Goldstein and Spores. The data of Goldstein and Spores were normalized so that at an $x/c_x = 0.2$ upstream of the leading edge the normalized value was unity. Part of the normalization accounted for the unheated starting length. This factor was 1.24 at the point where the normalized value was unity and decreased to 1.14 at the rotor trailing edge. Predictions were normalized in the same manner. In addition to the comparison of experimental Stanton numbers, the Stanton number based on inlet conditions is shown. The nature of the napthalene measurement technique allows for very detailed localized measurements. Both the measurements and predictions show very high heat transfer in front of the leading edge, with a peak ratio in excess of 3.25. The data show the peak passage heat transfer to occur near midpassage, and somewhat upstream of the throat region. The analysis tends to overpredict the heat transfer in the throat region, but does show the correct location of the peak passage heat transfer. Comparing the two calculations shows that normalizing the Stanton number to account for the starting length has only a small effect on the shape of the endwall heat transfer distribution.

The normalized comparison does not verify the absolute level of the predicted heat transfer. Goldstein and Spores gave the mass transfer Stanton number,St_m, as 1.472×10^{-3}, where the normalized value was unity. Heat transfer predictions were converted to mass transfer values using the relationship $St = St_m(Pr/Sc)^{n-1}$. Chen and Goldstein(1992) stated that $2.0 < Sc < 2.5$, and chose $n = 0.33$. Assuming $Sc = 2.0$ yields heat transfer Stanton numbers almost exactly twice the mass transfer Stanton numbers. This ratio gives a heat transfer Stanton numbers of 0.0029, where the St_m was 1.472×10^{-3} . The predicted Stanton number at the location where the experimental Stanton number ratio was unity was 0.003. This indicates good agreement between the analysis and the experimental data in terms of the Stanton number level in the leading edge region.

There were only small differences in the experimental data among the three cases. The agreement between the predictions and the data was better for the high Reynolds number cases. Allowing the near wall damping coefficient, A^+, to be a function of the pressure gradient did not improve the agreement with the data.

Figure 6b shows comparisons for the rotor heat transfer measured by Chen and Goldstein(1992). The experimental data were presented in terms of St_m values. The predicted St values were divided by 2 for comparison purposes. There is a two-dimensional region away from the endwall, and a three-dimensional region associated with the passage vortex. The experimental suction surface data show a line separating a high heat transfer region close to the endwall from the low Stanton number region towards midspan. The predictions show the same separation into two regions, but the demarcation line does not advance up the span as rapidly, and the peak value near the endwall is lower. Also, the predictions agree with the measurements in the leading edge region. In the measurements there is a high heat transfer region towards the trailing edge, but the predictions show low values in this region. Increasing the Tu level in the analysis moved transition forward, and gave high heat transfer in this region.

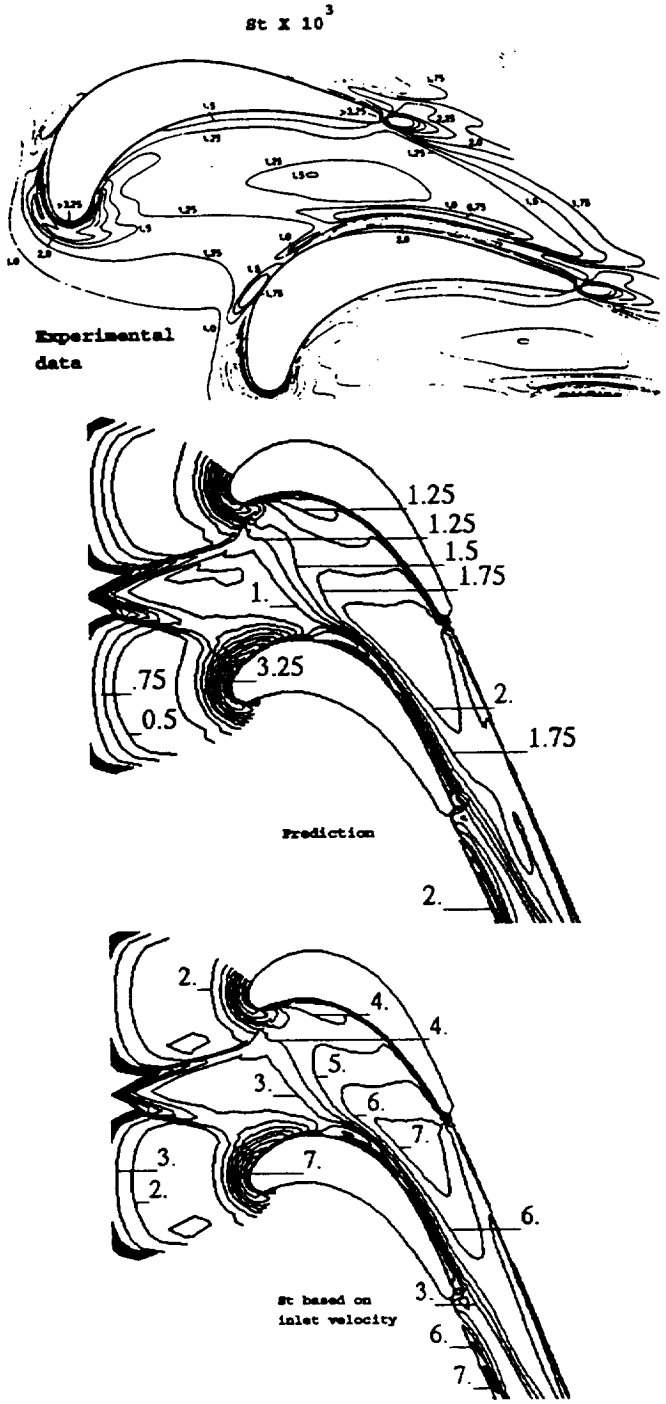

Fig. 6a - Stanton No. comparisons. Data of Goldstein and Spores, $Re_2 = 2.3 \times 10^5$, thin inlet boundary layer.

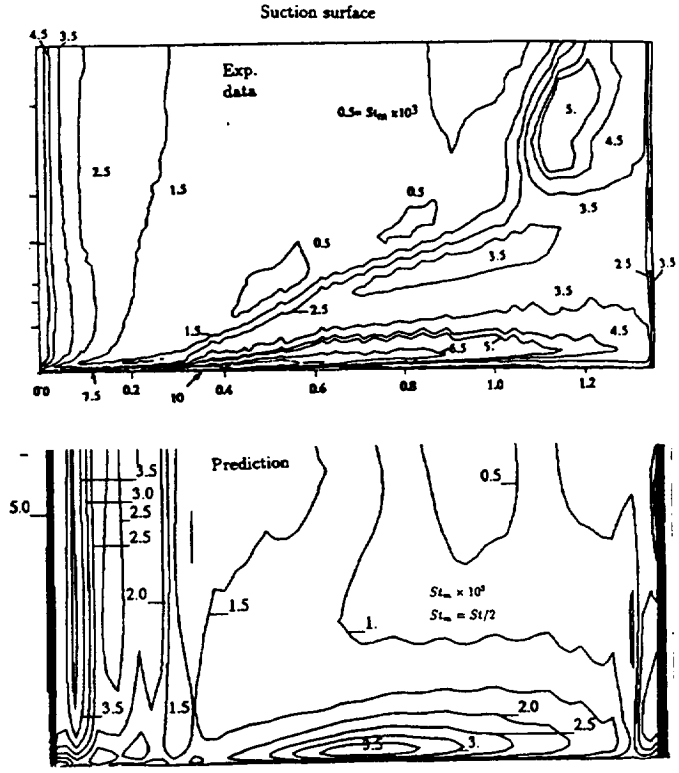

Fig. 6b - Stanton No. comparisons. Data of Chen and Goldstein.

Data of Blair. Figure 7 compares predicted and measured Stanton numbers for heat transfer to the hub and blade surface for two Reynolds numbers. The Stanton numbers are based on the rotor exit relative conditions. Even though the Reynolds number varied by a factor of three, the measured Stanton numbers are only slightly lower. The predictions are only moderately lower. The expected change is not to large since assuming $St \propto Re^{-0.2}$ gives only a 25% decrease in heat transfer for a factor of three increase in Re. There is good agreement with the data in the endwall leading edge region. The peak value predicted in the passage is somewhat greater than the experimental value, and agrees best for the high Reynolds number case. Although not shown in the measurements there is a peak predicted heat transfer level in the wake as great as the peak passage value.

The predicted rotor midspan heat transfer on the rear portion of the suction surface agrees well with the data. A Tu of 10% was used in the analysis, and resulted in transition closer to the leading edge than is evidenced by the data. The data show high heat transfer levels on the suction surface near the hub, and close to the tip, where the heat transfer is affected by the clearance flows. The analysis predicts these high heat transfer rates. In terms of the rotor hub region heat transfer, these results agree better with the data than do the predictions for the data of Chen and Goldstein(1992). The heat transfer predictions for the pressure surface are higher than the data. This is due to an early prediction for the start of transition.

Variations in the inlet flow angle did not affect the degree of agreement between the analysis and the data.

Data of Giel et al. Figure 8 compares predicted and measured Stanton numbers for two Reynolds numbers. The cases are for an $M_2 = 1.3$, and a low Tu. Predicted Stanton numbers are calculated in the same manner as the experimental

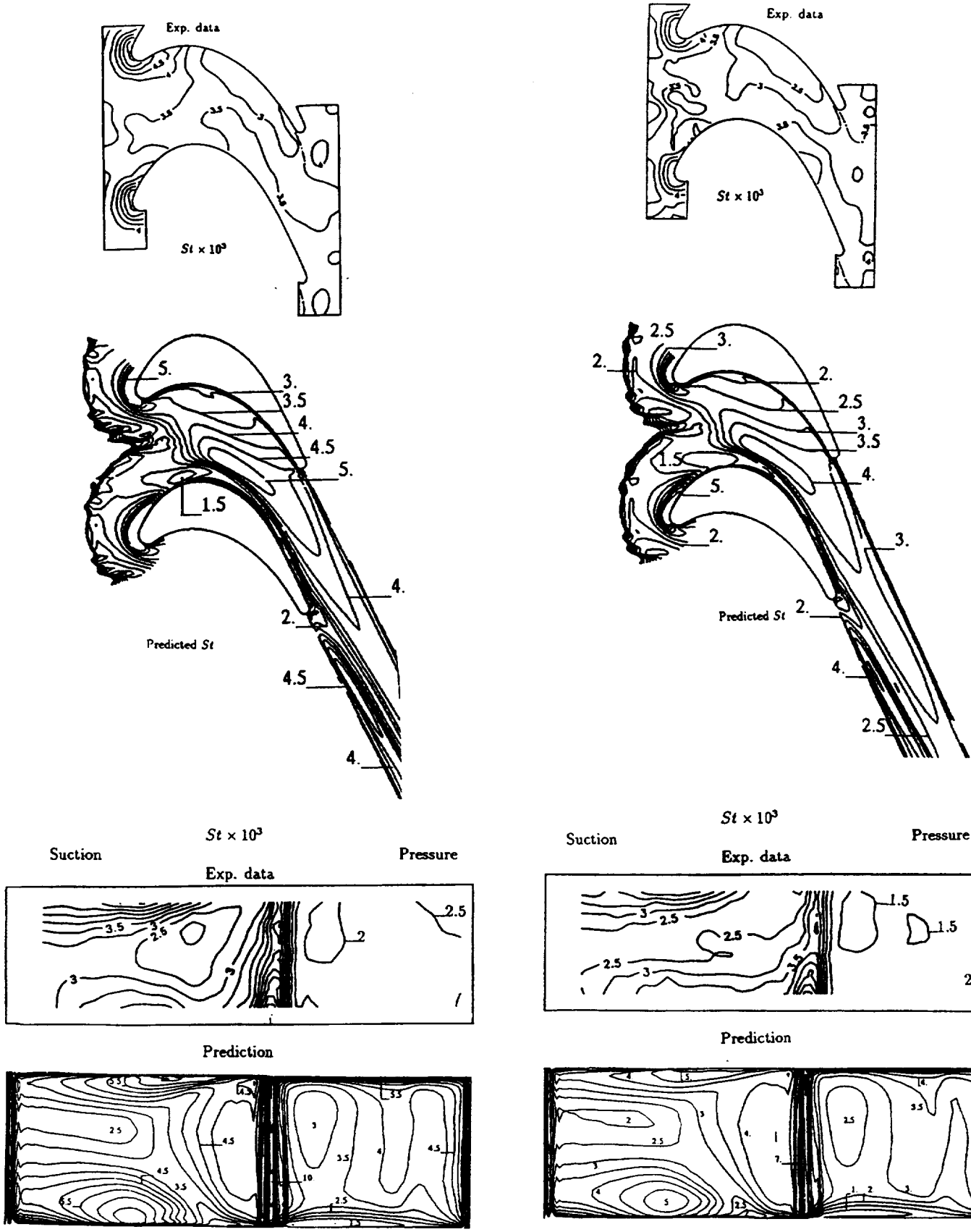

Fig. 7a- Stanton No. comparisons. Data of Blair, $Re_2 = 2.3 \times 10^5$

Fig. 7b- Stanton No. comparisons. Data of Blair, $Re_2 = 7.1 \times 10^5$

data, and is based on the calculated adiabatic wall temperature. In common with most of the previous comparisons, the agreement in the leading edge region is good. Within the passage the analysis shows a somewhat higher heat transfer level, but the correct trend in the distribution. The analysis, and especially the low Reynolds number data show what appears to be the effect of a separation line going from the pressure side leading edge region to midchord on the suction surface. In the data high heat transfer levels are seen upstream of this line, while the prediction show high levels immediately downstream of this line. Unlike several of the previous comparisons, the analysis fails to show very high heat transfer rates just downstream of the trailing edge. This may have been caused by insufficient grid resolution in this region.

Comparisons were made with the data of Giel et al. for cases in which the inlet boundary layer thickness was reduced, and in which the exit Mach number was reduced to 1.0. The reduced inlet boundary layer thickness resulted in reduced secondary flows. The measured endwall heat transfer near the pressure surface just upstream of the throat was lowered when there was a thinner inlet boundary layer. The analysis showed the same behavior. Reducing the exit Mach number gave slightly higher heat transfer downstream of the throat. This effect was also seen in the predictions.

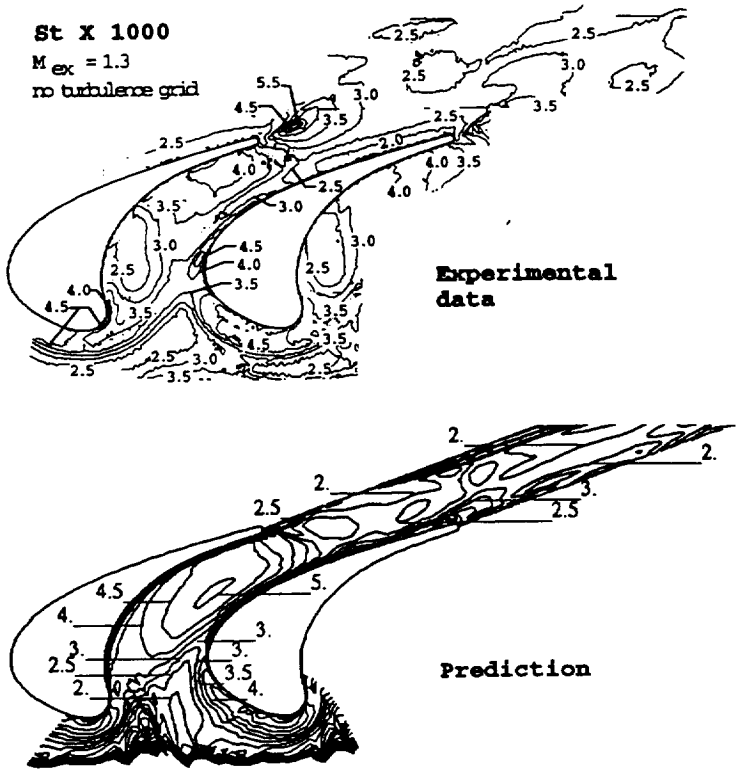

Fig. 8a. Stanton No. comparisons, Data of Giel et al., $Re_2 = 26 \times 10^5, M_2 = 1.3$

Turbulence model effects

All of the comparisons shown so far have been for the turbulence model described by Chima et al.(1993). The comparisons that were given showed the predicted heat transfer was generally higher than the measurements. For comparisons where T_w/T_g' was characteristic of engine operating conditions, the degree of overprediction was small. For comparisons where T_w/T_g' was small, and the Mach number was low, the degree of overprediction was high. The primary cause of these results is the choice of turbulence model. Results presented in this section illustrate the effects of an alternative algebraic turbulence model on heat transfer predictions. These comparisons illustrate the sensitivity of the heat transfer predictions to the choice of turbulence model. The predictions shown in this section were obtained using the Baldwin-Lomax(1978) turbulence model. Predictions shown using this model will be labeled as Baldwin-Lomax results. The following figures illustrate the differences in heat transfer attributable solely to differences in the turbulence models.

Figure 9 shows the prediction using the Baldwin-Lomax turbulence model for the same test case as in figure 2b. The Stanton numbers are in better agreement with the data using the Baldwin-Lomax model. The peak endwall heat transfer has been reduced considerably, and is in closer agreement with the experimental data.

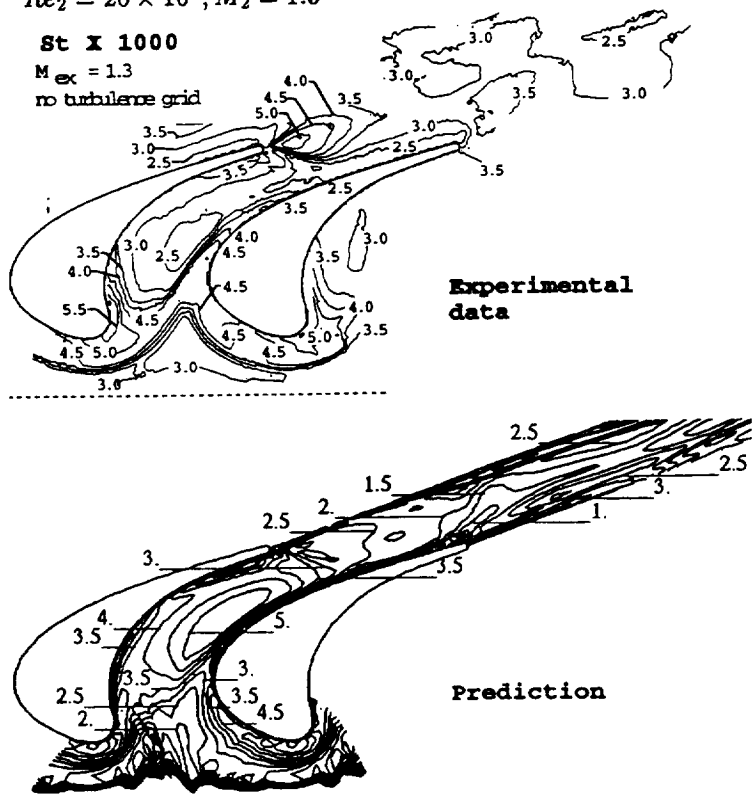

Fig. 8b. Stanton No. comparisons, Data of Giel et al., $Re_2 = 13 \times 10^5, M_2 = 1.3$

Figure 10 shows prediction using the Baldwin-Lomax model for the test case in figure 3. Only the hub endwall prediction is shown. The relative differences between the two predictions were the same for the hub and tip. The vane surface prediction in figure 10 shows better agreement with the presssure and suction surface data than the comparison shown in figure 3c. There are differences in the vane suction surface heat transfer between the two predictions. The predictions in figure 10 were calculated assuming the turbulence intensity remained constant. This caused the start of transition to move forward on the suction surface. The data indicate that the assumption of variable turbulence intensity gives better agreement for the transition location. The hub heat transfer prediction using the Baldwin-Lomax model does not agree with the experimental results better than the prediction using Chima's turbulence model. The predictions using the Baldwin-Lomax model are significantly lower near the vane suction surface beyond the throat.

Figure 11 shows the prediction for design condition used by Harasagama and Wedlake(1991). These results should be compared with the data in figure 4a. The effect of varying the turbulence Model for this test case are very similar to the results shown in the previous figure for the data of Arts and Heider. The vane surface heat transfer prediction is somewhat improved, but the endwall heat transfer prediction agrees less well with the experimental data.

There is a high degree of similarity between the predictions for the data of Goldstein and Spores, and for the data of Graziani et al.(1980). The effects of varying the turbulence model were the same for the two configurations. Figure 12 shows the hub and rotor surface predictions for the same case as given in figure 5. Somewhat surprisingly, substituting the Baldwin-Lomax turbulence model has only a small effect on the endwall heat transfer. The predicted heat transfer is still significantly higher than the data. The results shown in figure 12 for the vane surface illustrate two independent effects. For the suction surface the figure illustrates the effect of a different turbulence model. The effects are small. For the pressure surface figure 12 illustrates the effect of suppressing transition. A laminar calculation for the pressure surface is in good agreement with the experimental data.

Using the Baldwin-Lomax turbulence model to predicted the high Reynolds number rotor test case of Blair(1994) is illustrated in figure 13. These results should be compared with those shown in figure 7b. Here the effect of varying the turbulence model is relatively small. The flow distribution determined for a rotating blade with clearance appears to have the dominant effect on surface heat transfer.

Figure 14 illustrates the effect of using the Baldwin-Lomax turbulence model for the high Reynolds number test case of Giel et al. These predictions should be compared with the results in figure 8a. These heat transfer rates are lower than those calculated using Chima's turbulence model. Chima's model gives heat transfer rates that are in better agreement with the experimental data.

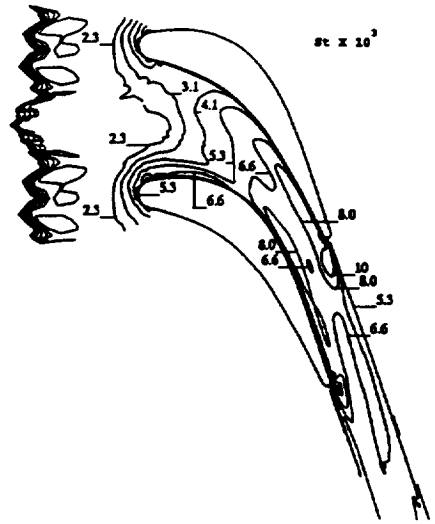

Fig. 9. Prediction of high Reynolds number case of Boyle and Russell with Baldwin-Lomax turbulence model.

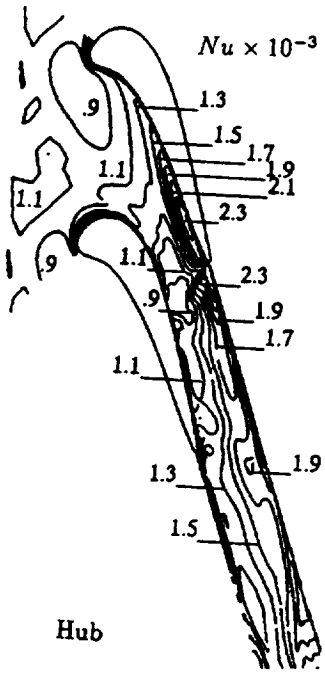

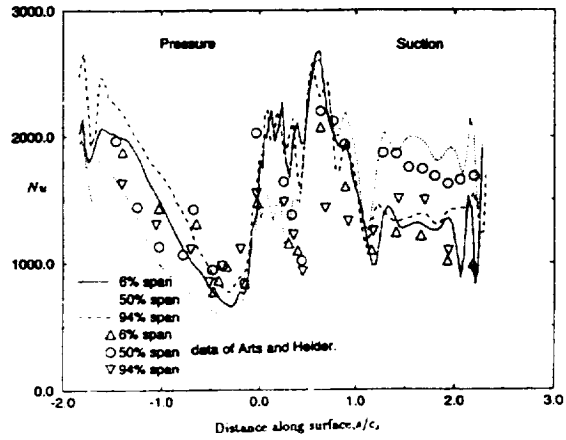

Fig. 10. Prediction of Arts and Heider case with Baldwin-Lomax turbulence model.

Both Chima's turbulence model and the Baldwin-Lomax model are two layer models, and have the same inner layer formulation. The outer layer eddy viscosity is determined differently in each model. These differences, which are described by Chima et al.(1993), give rise to the differences in the heat transfer predictions. Greater outer layer eddy viscosities are associated with higher heat transfer rates. Increased outer layer eddy viscosities result from increased wall distances at which the outer layer values are determined.

CONCLUDING REMARKS

Comparisons were shown between predicted and measured blade and endwall heat transfer for data obtained from a variety of sources. Unfortunately, one turbulence model did not give good agreement for all cases. For all of the cases examined the baseline model gave peak heat transfer rates as high or higher than the measured values. Those cases for which the wall-to-gas temperature ratio was characteristic of actual engine conditions had predicted heat transfer rates in good agreement with the data overall. The predictions were only slightly higher on the endwall at the peak location in the throat region. Overall, the model was conservative in that it gave higher than measured heat transfer rates.

Comparisons for cases with wall-to-gas temperature ratios not typical of actual engine operation, and low Mach numbers showed that the baseline turbulence model was conservative, perhaps to an unacceptably high degree. An alternate turbulence model gave reasonably good heat transfer predictions for these test cases. However, this model underpredicted the heat transfer for cases with wall-to-gas temperature ratios representative of actual engine operation.

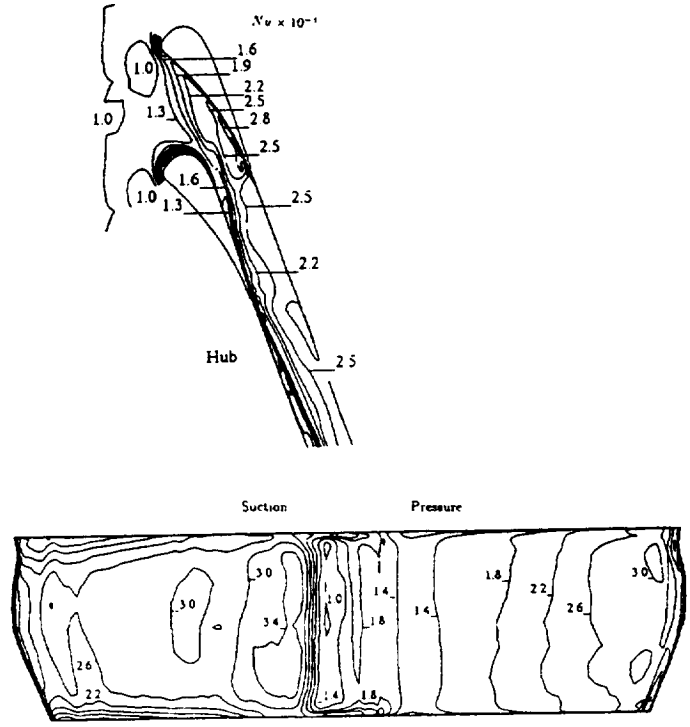

Fig. 11 Prediction of high *Re* case of Harasagama and Wedlake with Baldwin-Lomax turbulence model.

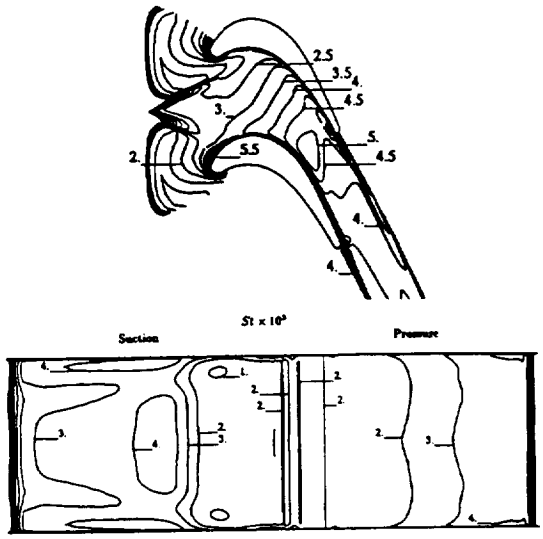

Fig. 12. Prediction of Graziani et al. with Baldwin-Lomax turbulence model.

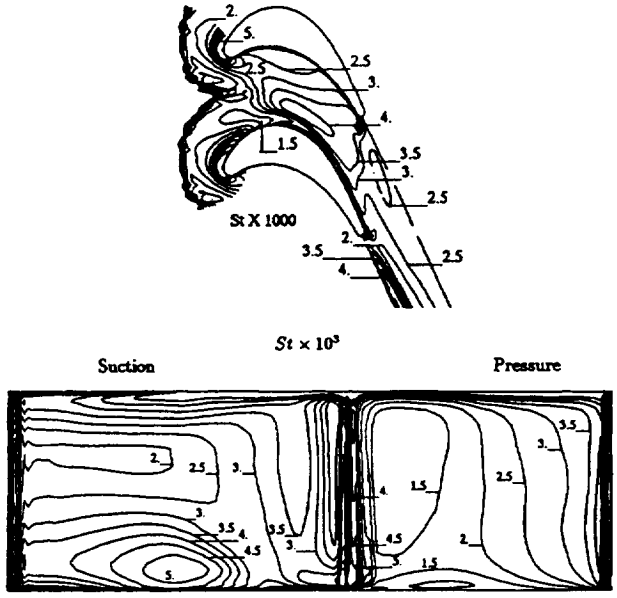

Fig. 13. Prediction of Blair's high *Re* case with Baldwin-Lomax turbulence model.

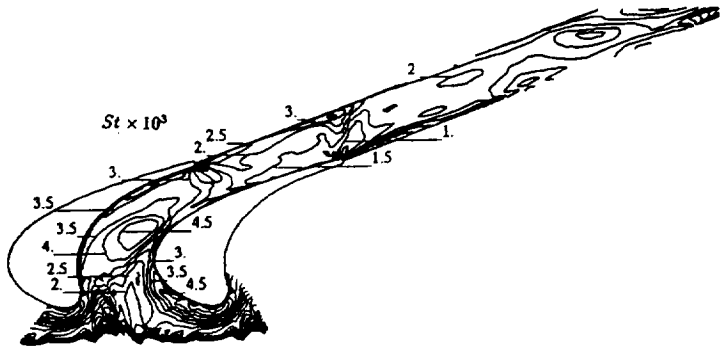

Fig. 14 Prediction of high Reynolds number case of Giel et al. with Baldwin-Lomax turbulence model.

REFERENCES

Ameri, A.A. and Arnone, A., 1994, "Prediction of Turbine Blade Passage Heat Transfer Using a Zero and a Two-Equation Turbulent Model," ASME Paper 94-GT-122.

Arnone, A, Liou, M.-S, and Povinelli, L. A., 1992, "Navier-Stokes Solution of Transonic Cascade Flows Using Non-Periodic C-Type Grids," AIAA *Journal of Propulsion and Power*, Vol. 8, No.2, pp 410-417.

Arts, T, and Heider, R., 1994, "Aerodynamic and Thermal Performance of a Three Dimensional Annular Transonic Nozzle Guide Vane. Part I: Experimental Investigation," AIAA Paper AIAA-94-2929.

Baldwin, B.S. and Lomax, H., 1978, "Thin- Layer Approximation and Algebraic Model for Separated Turbulent Flows," AIAA Paper AIAA-78-257.

Blair, M. F., 1974, "An Experimental Study of Heat Transfer and Film Cooling in Large-Scale Turbine Endwalls," ASME *Journal of Heat Transfer*, Vol 96, pp.525-529, 1974.

Blair, M. F., 1994, "An Experimental Study of Heat Transfer in a Large-Scale Turbine Rotor Passage," ASME *Journal of Turbomachinery*, Vol. 116, No. 1, pp 1-13.

Boyle, R. J, and Russell, L. M., 1990, "An Experimental Determination of Stator Endwall Heat Transfer," ASME *Journal of Turbomachinery*, Vol 112, pp.547-558.

Boyle, R. J, and Jackson, R., 1995,"Heat Transfer Predictions for Two Turbine Nozzle Geometries at High Reynolds and Mach Numbers," ASME paper 95-GT-104.

Boyle, R.J., and Giel, P.W., 1992, "Three-Dimensional Navier-Stokes Heat Transfer Predictions for Turbine Blade Rows," AIAA paper AIAA-92-3068.

Boyle, R.J., and Ameri, A., 1994, "Grid Orthogonality Effects onPredicted Turbine Midspan Heat Transfer and Performance," ASME paper 94-GT-123.

Cebeci, T., and Smith, A.M.O., 1974, "*Analysis of Turbulent Boundary Layers*, Acedemic Press, New York.

Chen, P.H., and Goldstein, R. J., 1992, "Convective Transport Phenomena on the Suction Surface of a Turbine Blade Including the Influence of Secondary Flows Near the Endwall," ASME *Journal of Turbomachinery*, Vol 114, No. 4, pp.776-787.

Chana, K.S., 1992, "Heat Transfer and Aerodynamics of a High Rim Speed Turbine Nozzle Guide Vane with Profiles End Walls," ASME paper 92-GT-243.

Chima, R.V., and Yokota, J.W., 1988, "Numerical Analysis of Three-Dimensional Viscous Internal Flows," AIAA paper 88-3522, (NASA TM-100878).

Chima, R.V., 1991, "Viscous Three-Dimensional Calculations of Transonic Fan Performance," AGARD Propulsion and Energetics Symposium on Computational Fluid Mechanics for Propulsion, San Antonio, Texas, May 27-31.

Chima, R.V., Giel, P.W., and Boyle, R.J., 1993, "An Algebraic Turbulence Model for Three-Dimensional Viscous Flows," AAIA paper 93-0083, (NASA TM-105931).

Choi, D., and Knight, C.J., 1988, "Computations of 3D Viscous Linear Cascade Flows," AIAA *Journal* Vol. 26, No. 12, pp 1477-1482.

Georgiou, D. P., Godard, M., and Richards, B. E., 1979, "Experimental Study of the Iso-Heat-Transfer-Rate Lines on the End-Wall of a Turbine Cascade," ASME paper 79-GT-20.

Giel, P.W., Thurman, D.R., Van Fossen, G.J., Hippensteele, S.A., and Boyle, R.J., 1996, "Endwall Heat Transfer Measurements in a Transonic Turbine Cascade," To be presented at the ASME Gas Turbine Conference, June 10-13, Birmingham, UK.

Goldstein, R.J., and Spores, R.A., 1988 "Turbulent Transport on the Endwall in the Region Between Adjacent Turbine Blades", ASME *Journal of Heat Transfer*, Vol. 110, No. 4, pp 862-869.

Graziani, R.A., Blair, M.F., Taylor, R.J., and Mayle, R.E., 1980, "An Experimental Study of Endwall and Airfoil Surface Heat Transfer in a Large Scale Turbine Blade Cascade," *Journal of Engineering for Power*, Vol. 102, No. 2, pp. 1-11.

Hah, C., 1989,"Numerical Study of Three-Diensional Flow and Heat Transfer Near the Endwall of a Turbine Blade Row," AIAA paper 89-1689.

Harasagama, S.P., Wedlake, E.T., 1991, "Heat Transfer and Aerodynamics of a High Rim Speed Turbine Nozzle Guide Vane Tested in the RAE Isentropic Light Piston Cascade(ILPC)," ASME *Journal of Turbomachinery*, Vol. 113, No. 4, pp 384-391.

Heider, R. and Arts, T., 1994, "Aerodynamic and Thermal Performance of a Three Dimensional Annular Transonic Nozzle Guide Vane. Part II: Assessment of a 3D Navier-Stokes Solver," AIAA Paper AIAA-94-2930.

Hylton, L. D., Mihelc, M. S., Turner, E. R., York, R. E., 1981, "Experimental Investigation of Turbine Endwall Heat Transfer," Detroit Diesel Allison Report EDR 10363, Volumes I-III, (Aero Propulsion Laboratory Report AFWAL-TR-81-2077, Volumes I-III.)

Kays, W.M., Crawford, M.E., *Convective Heat and Mass Transfer*, McGraw-Hill Pub. Co., 1980.

Mayle, R.E., 1991, "The role of Laminar-Turbulent Transition in Gas Turbine Engines," ASME *Journal of Turbomachinery*, Vol. 113, pp 509-537.

Smith, M.C., and Kuethe, A.M., 1966, "Effects of Turbulence on Laminar Skin Friction and Heat Transfer," Physics of Fluids, Vol. 9, pp. 2337-2344.

Sorenson, R.L., 1980, "A Computer Program to Generate Two-Dimensional Grids About Airfoils and Other Shapes by the Use of Poisson's Equation,", NASA TM 81198.

York, R. E., Hylton, L.D., and Mihelc, M. S., 1984, "Experimental Endwall Heat Transfer and Aerodynamics in a Linear Vane Cascade," ASME *Journal of Engineering for Gas Turbines and Power*, Vol 106, pp.159-167.

REPORT DOCUMENTATION PAGE

Form Approved
OMB No. 0704-0188

1. AGENCY USE ONLY (*Leave blank*)	2. REPORT DATE	3. REPORT TYPE AND DATES COVERED
	November 1996	Technical Memorandum

4. TITLE AND SUBTITLE

Predicted Turbine Heat Transfer for a Range of Test Conditions

5. FUNDING NUMBERS

WU-505-62-52

6. AUTHOR(S)

R.J. Boyle and B.L. Lucci

7. PERFORMING ORGANIZATION NAME(S) AND ADDRESS(ES)

National Aeronautics and Space Administration
Lewis Research Center
Cleveland, Ohio 44135-3191

8. PERFORMING ORGANIZATION REPORT NUMBER

E-10543

9. SPONSORING/MONITORING AGENCY NAME(S) AND ADDRESS(ES)

National Aeronautics and Space Administration
Washington, D.C. 20546-0001

10. SPONSORING/MONITORING AGENCY REPORT NUMBER

NASA TM-107374

11. SUPPLEMENTARY NOTES

Prepared for the 41st Gas Turbine and Aeroengine Congress sponsored by the International Gas Turbine Institute of the American Society of Mechanical Engineers, Birmingham, United Kingdom, June 10-13, 1996. Responsible person, R.J. Boyle, organization code 2640, (216) 433-5889.

12a. DISTRIBUTION/AVAILABILITY STATEMENT

Unclassified - Unlimited
Subject Category 34

This publication is available from the NASA Center for AeroSpace Information, (301) 621-0390.

12b. DISTRIBUTION CODE

13. ABSTRACT (*Maximum 200 words*)

Comparisons are shown between predictions and experimental data for blade and endwall heat transfer. The comparisons are given for both vane and rotor geometries over an extensive range of Reynolds and Mach numbers. Comparisons are made with experimental data from a variety of sources. A number of turbulence models are available for predicting blade surface heat transfer, as well as aerodynamic performance. The results of an investigation to determine the turbulence model which gives the best agreement with experimental data over a wide range of test conditions are presented.

14. SUBJECT TERMS

Turbine; Heat transfer; Navier-Stokes

15. NUMBER OF PAGES

18

16. PRICE CODE

A03

17. SECURITY CLASSIFICATION OF REPORT	18. SECURITY CLASSIFICATION OF THIS PAGE	19. SECURITY CLASSIFICATION OF ABSTRACT	20. LIMITATION OF ABSTRACT
Unclassified	Unclassified	Unclassified	

National Aeronautics and
Space Administration

Lewis Research Center
21000 Brookpark Rd.
Cleveland, OH 44135-3191

NASA Technical Memorandum 107374

Predicted Turbine Heat Transfer for a Range of Test Conditions

R.J. Boyle and B.L. Lucci
Lewis Research Center
Cleveland, Ohio

Prepared for the
41st Gas Turbine and Aeroengine Congress
sponsored by the International Gas Turbine Institute of
the American Society of Mechanical Engineers
Birmingham, United Kingdom, June 10–13, 1996

National Aeronautics and
Space Administration

PREDICTED TURBINE HEAT TRANSFER FOR A RANGE OF TEST CONDITIONS

R. J. Boyle
NASA Lewis Research Center
Cleveland, OH 44135

B. L. Lucci
NASA Lewis Research Center
Cleveland, OH 44135

ABSTRACT

Comparisons are shown between predictions and experimental data for blade and endwall heat transfer. The comparisons are given for both vane and rotor geometries over an extensive range of Reynolds and Mach numbers. Comparisons are made with experimental data from a variety of sources. A number of turbulence models are available for predicting blade surface heat transfer, as well as aerodynamic performance. The results of an investigation to determine the turbulence model which gives the best agreement with experimental data over a wide range of test conditions are presented.

Nomenclature

c	-	True chord
c_x	-	Axial chord
c_p	-	Specific heat
d	-	Distance from surface
h	-	Span
Ec	-	Eckert number, $W_2^2/c_p/\|(T_g' - T_w)\|$
M_2	-	Isentropic exit relative Mach No.
Nu	-	Nusselt No. based on true chord and $k(T_1')$
P	-	Pressure
Pr	-	Prandlt No.
Pr_t	-	Turbulent Prandlt No.
Re_2	-	Reynolds No. based on true chord and M_2
Sc	-	Schmidt number
St	-	Stanton number
St_m	-	Mass transfer Stanton number
s	-	Surface distance
T	-	Temperature
Tu	-	Turbulence intensity
W	-	Relative velocity
y_1^+	-	Normalized distance of first grid line from blade
δ	-	Inlet boundary layer thickness
μ_t	-	Turbulent eddy viscosity
ρ	-	Density

Subscripts

EXIT	-	Exit of computational domain
f	-	Full
g	-	Gas total condition
w	-	Surface
1	-	inlet
2	-	outlet

INTRODUCTION

A relatively large number of three-dimensional Navier-Stokes analyses for turbine blade row heat transfer have been reported in the literature. Each of the reported results have shown comparisons with at most a few experimental cases. In order to validate an approach to predicting turbine blade row heat transfer, it is desirable to show comparisons with experimental data for an extended range of test conditions. Among the earliest heat transfer predictions using steady state three-dimensional analyses were those of Hah(1989) and Choi and Knight(1988). They showed comparisons with the experimental data of Graziani et al.(1980). The experimental data were for a large scale rotor geometry tested in a linear cascade at low Mach number. The tests were conducted with a uniform heat flux boundary condition which resulted in an average T_w/T_g' of approximately 1.08. Chima et al.(1993) showed comparisons of endwall heat transfer predictions with the experimental data of Boyle and Russell(1990). Again, the experimental data were for a large scale, relatively low speed linear cascade, with low turbulence intensity and a $T_w/T_g' = 1.07$. Data have been obtained on a large scale rotating turbine rotor by Blair(1994). These data were for a variety of Reynolds numbers and incidence angles. In these tests the Mach numbers were relatively low, and the average $T_w/T_g' = 1.1$. Data for stator vanes at transonic Mach numbers and wall-to-gas temperature ratios typical of gas turbine applications have been measured by a number of researchers. York et al.(1984) obtained data in a linear cascade for a

Table I. - Description of cases used in analysis

Vanes					
Source of data	$Re_{2c}X10^{-5}$	M_{EXIT}	T_w/T_g'	Cascade	Test approach
York et al.(1984)	2.1-18.0	0.3-1.1	0.75	Linear	Steady state
Arts and Heider(1994)	22.5	0.92-1.15	0.73	Annular	Shock tube
Boyle and Russell(1990)	3.4-20	0.1-0.7	1.1	Linear	Liquid Crystals
Harasagama and Wedlake(1990)	17-52	0.94-1.29	0.66	Annular	Shock tube
Rotors					
Source of data	$Re_{2c}X10^{-5}$	M_{EXIT}	T_w/T_g'	Cascade	Test approach
Blair(1994)	2.7-7.1	0.06-0.15	1.1	Rotating	Steady state
Goldstein and Spores(1988)	1.4-2.3	0.03-0.04	1	Linear	Napthalene
Chen and Goldstein(1992)	1.2-2.0	0.02-0.03	1	Linear	Napthalene
Graziani et al.(1980)	10.7	0.1	1.1	Linear	Steady state
Giel et al.(1996)	13-26	1.0-1.3	1.1	Linear	Steady state

Table II. - Characteristics of experimental data

Vanes						
Source of data	$Tu\%$	Heat Transfer		$(T_w)_1/T_g'$	Ec	No. of
		Endwall	Blade			Cases
York et al.(1984)	7.0	Y	N	1.0	1.56	4
Arts and Heider(1994)	4.5	Y	Y	0.73	1.56	1
Boyle and Russell(1990)	1.0	Y	N	1.0	1.51	2
Harasagama and Wedlake(1990)	6.5	Y	Y	0.66	1.47	5
Rotors						
Source of data	$Tu\%$	Heat Transfer		$(T_w)_1/T_g'$	Ec	No. of
		Endwall	Blade			Cases
Blair(1994)	High	Y	Y	1.0	0.15	3
Goldstein and Spores(1988)	1.2	Y	N	1.0	N.A.	3
Chen and Goldstein(1992)	1.2	N	Y	1.0	N.A.	1
Graziani et al.(1980)	1	Y	Y	1.0	0.18	2
Giel et al.(1995)	0.3-7	Y	N	1.0	5.3-8	4

stator vane configuration. Harasagama and Wedlake(1991), Chana(1992), and Arts and Heider(1994) presented stator vane heat transfer obtained in shock tube facilities for annular cascades. Predictions using three-dimensional Navier-Stokes analyses were obtained by Heider and Arts(1994) for the data of Arts and Heider(1994), and by Boyle and Jackson(1995) for the data of Chana(1994).

In general most predictions presented in the literature showed comparisons with a limited number of experimental cases. The data available in the literature cover a wide variety of test conditions. In addition to a range of geometries, Reynolds and Mach numbers, there are significant differences in turbulence intensity, inlet boundary layer thicknesses, as well as inlet blade row temperature profile among the experimental data.

The work reported herein consists of comparisons of predicted blade row heat transfer with experimental data for a variety of test configurations. The purpose of examining a variety of test configurations is to increase confidence in the ability of both the analysis and turbulence model to predict blade row heat transfer. The analysis was done using the steady state three-dimensional Navier-Stokes code described by Chima(1991), and by Chima and Yokota(1988). Results were obtained using algebraic turbulence models.

EXPERIMENTAL DATA USED FOR VERIFICATION

Table I gives a description of the experimental data sources with which the computational results are compared. There are four stator and four rotor geometries. The data of Goldstein and Spores(1988) are for the same rotor geometry as Chen and Goldstein(1992). The maximum Mach number for each of the stator tests is in the transonic flow regime, but only the rotor test data of Giel et al.(1996) is in the transonic region. Except for the data of Graziani et al.(1980), the

Table III. - Characteristics of cases examined

Vanes									
Source of data	c_x,(cm)	c_t/c_x	h/c_x	δ_f/c_x	Re_2X10^{-5}	Re_1/Re_2	P_2/P_1'	y_1/c_x	$(T_w)_1/T_g'$
York et al.(1984)	5.25	1.775	1.45	0.12	2.1	0.36	0.951	2.8e-05	1.0
				0.12	6.2	0.32	0.721	2.2e-05	1.0
				0.12	18.0	0.32	0.721	8.0e-06	1.0
				0.12	18.0	0.30	0.468	7.4e-06	1.0
Arts and Heider(1994)	4.21	1.836	1.19	0.0012	22.5	0.25	0.440	1.0e-05	0.73
Boyle and Russell(1990)	13.8	1.393	1.104	0.184	3.4	0.35	0.996	0.9e-04	1.0
				0.184	20.0	0.35	0.836	1.8e-05	1.0
Harasagama and	3.96	1.881	1.26	0.093	34.0	0.25	0.566	5.6e-06	0.659
Wedlake(1990)					34.0	0.24	0.445	5.0e-06	0.659
					34.0	0.23	0.366	4.7e-06	0.659
					17.0	0.24	0.445	9.4e-06	0.659
					52.0	0.24	0.445	3.4e-06	0.659

Rotors									
Source of data	c_x,(cm)	c_t/c_x	h/c_x	δ_f/c_x	Re_2X10^{-5}	Re_1/Re_2	P_{EXIT}	y_1/c_x	$(T_w)_1/T_g'$
Blair(1994)	16.1	1.22	0.946	0.05	2.7	0.59	0.997	1.0e-04	1.0
				0.05	2.7	0.78	0.997	1.0e-04	1.0
				0.05	7.1	0.78	0.980	1.0e-04	1.0
Goldstein and	14.53	1.1641	2.065	0.10	2.3	0.61	0.998	1.0e-04	1
Spores(1988)				0.20	2.3	0.61	0.998	1.0e-04	1
				0.08	1.4	0.61	0.999	1.5e-04	1
Chen and Goldstein(1992)	14.53	1.1641	2.065	0.18	2.0	0.61	0.998	1.0e-04	1
Graziani et al.(1980)	28.13	1.22	0.99	0.014	10.8	0.63	0.985	3.0e-05	1.0
				0.117	10.8	0.63	0.985	3.0e-05	1.0
Giel et al.(1996)	12.7	1.45	1.20	0.24	26.	0.53	0.361	7.4e-06	1.00
				0.27	13.	0.53	0.361	1.4e-05	1.00
				0.15	26.	0.53	0.361	7.4e-06	1.00
				0.24	26.	0.53	0.528	8.9e-06	1.00

low Mach numbers are associated with low Reynolds numbers. Except for the data of Boyle and Russell(1990), the stator data are all for T_w/T_g' values representative of actual engine applications. The data for rotor geometries are all for T_w/T_g' close to unity. Data obtained using liquid crystals or Napthalene permit near continuous measurement of the surface heat transfer. Blair(1994) obtained data in a rotating large scale facility for a range of incidences.

Table II gives characteristics of the various data sources. The data of Boyle and Russell(1990) were for a low turbulence intensity, while the other stator data were for moderate to high levels of turbulence. All cases had endwall data, and Arts and Heider(1994) and Harasagama and Wedlake(1990) showed vane heat transfer data. High turbulence levels were present in Blair's test and for some of the tests of Giel et al. The other rotor data had low turbulence levels.

Table II also lists the Eckert,Ec, numbers for each data source. The values shown are for the maximum blade row exit velocity for each data set. The Ec number indicates the importance of viscous dissipation in determining the near wall temperature profile. All of the stator test cases have maximum Ec numbers greater than one, while only the rotor cases of Giel et al. had Ec values greater than 0.2. Because the cases with wall-to-gas temperature ratios representative of actual engine conditions also have high exit Mach numbers, these cases also have relatively high Eckert numbers.

Table III shows geometric, flow, and thermal characteristics of the various cases examined. The inlet and exit Reynolds numbers are shown for each test case. Both Reynolds numbers are given to facilitate comparisons among different investigators. Some experimental heat transfer results were given using inlet conditions, while others used exit conditions. Those cases where the inlet wall temperature ratio,$(T_w)_1/T_g'$, is given as unity have unheated,(or uncooled in the case of York et al.), starting lengths. This table also shows the near wall spacing used in the computational analysis. This is the spacing of the first grid line from either the blade or endwall surface. This spacing, y_1/c_x, was determined from a flat plate correlation so as to give a y_1^+ of approximately one.

DESCRIPTION OF COMPUTATIONAL ANALYSIS

Steady state heat transfer predictions were made using the three-dimensional Navier-Stokes computer code RVC3D. This code is a finite difference analysis, and was described by Chima(1991), and by Chima and Yokota(1988). The analysis used a Runge-Kutta time marching approach. Implicit residual smoothing is used to improve convergence. Three algebraic turbulence models are available for use in the code. These models can be viewed as variations of the commonly used Baldwin-Lomax(1978) algebraic turbulence model. Cases were run using each of the three turbulence models. Results are presented herein for the turbulence model which gave the best agreement with experimental data overall. The model chosen is the one described by Chima et al.(1993). Predictions using an alternative turbulence model are given for selected cases.

Since many of these test cases, and actual engine operation, were at relatively high turbulence levels, the transition criteria of Mayle(1991) was incorporated into the turbulence model. The Baldwin-Lomax transition criteria does not account for freestream turbulence effects. High freestream turbulence results in leading edge Frossling numbers significantly greater than unity. To account for the effect of freestream turbulence on laminar heat transfer, the model of Smith and Kuethe(1966) was incorporated into the calculation of turbulent viscosity.

Researchers showed good agreement between predicted and measured turbine blade heat transfer using both algebraic and two-equation turbulence models. For example, the experimental cascade data of Graziani et al.(1980) have been used for a number of different heat transfer predictions. Hah(1989), and Choi and Knight(1988) used two-equations turbulence models to predict the blade and endwall heat transfer. Ameri and Arnone(1994) analyzed this case using both two-equation and algebraic turbulence models. All of the predictions agree reasonably well with the experimental data. The aforementioned experimental case, along with several other available in the literature, is for low Mach number flow. It remains to be seen if algebraic models are as effective as two equation models in predicting turbine blade heat transfer for high Mach and Reynolds number cases. As shown by Ameri and Arnone(1994), heat transfer predictions using two-equation models required nearly twice the CPU time to converge, compared with an algebraic model solution. Results are presented herein for high Reynolds number cases, which require a moderate to large number of grid points. Since two equation turbulence models have not demonstrated a significant superiority over algebraic models for turbine blade heat transfer predictions, and CPU time is a significant consideration, algebraic turbulence models were used. Both Pr and Pr_t were held constant at 0.70 and 0.90 respectively.

A uniform temperature boundary condition was imposed on all solid boundaries. Spanwise radial equilibrium was assumed at the exit boundary. At each spanwise location the exit static pressure was allowed to vary in the circumferential direction. The average hub exit static pressure was specified, but the pitchwise variation was determined from the internal flow field. Uniform total conditions were specified for the inlet core flow, and uniform static pressures were specified through the boundary layers. The inlet boundary layer temperature and velocity profiles were determined using flat plate correlations in which the friction factor and Stanton number are determined by the specified inlet boundary layer thickness. The correlations are those given by Kays and Crawford(1980). Using a simple power law for the inlet temperature profile produces an erroneous result, since the power law gives an infinite gradient at the wall.

A large number of cases were examined, placing a premium on obtaing solutions with a minimum of CPU time. Therefore, moderate size grids were used. A typical grid size was $185 \times 49 \times 65$, and was chosen based on previous work, (Boyle and Giel(1992)). Even though midspan symmetry was assumed for the linear geometry test cases, 65 spanwise grid lines were used to maintain a desirable stretching ratio for the high Reynolds number test cases. C-type grids were generated using the procedure described by Arnone et. al.(1992). In this procedure grid lines near the surfaces are embedded within a coarse grid, which is generated using Sorenson's(1980) technique. It was found necessary to maintain grid stretching ratios less than 1.3 in addition to having a y_1^+ near unity to obtain grid independent results.

The primary convergence criteria was that the surface heat transfer remained constant as the solution advanced in time. It was observed that the ratio of inlet to exit mass flow varied greatly during the first five hundred or so iterations. In addition to the stability in the surface heat transfer, cases were run until there was only a small variation between the inlet and exit mass flow. When these criteria were met, it was found that the residuals had decreased by three or more orders of magnitude. The analysis was run on a Cray C90 machine. The CPU time for convergence was between one and three hours, with the low Mach number cases requiring the most time. The low Mach number cases were run with a minimum P_2/P_1' of 0.985 and the experimental Reynolds number to improve convergence speed. A test case with a higher pressure ratio, and the same Reynolds number took significantly longer to converge to the same result. The computer code was vectorized by the developer, Chima(1991). Consequently, the average CPU time per grid point to advance the solution one time cycle was 6×10^{-6} seconds.

DISCUSSION of RESULTS

Table II shows that 25 cases were examined. Only selected cases will be compared graphically, although the predictions for all cases will be discussed.

Vanes

Comparison with data of York et al.(1984) The data of York et al.(1984) were for a range of test conditions, but results were presented for only a single representative case. The report by Hylton et al.(1981) contained the data for the test matrix. Heat transfer coefficients were presented in terms of Stanton number based on local conditions. Figure 1 shows comparisons between the predicted and measured Stanton numbers for the $M_2 = 0.27$ and $Re_2 = 2.1 \times 10^5$ case, and the $M_2 = 1.1$, and $Re_2 = 18. \times 10^5$ case. The Stanton number based on inlet conditions is also given for the higher Mach number case. It is included to facilitate comparisons with data from other sources. In this plot a percentage variation in Stanton number represents the same percentage variation in heat transfer coefficient.

The predictions, and to some extent the experimental data, show very high values close to the leading edge of the pressure surface. This is a result of the Stanton number definition used. These high Stanton numbers do not represent regions of high heat transfer coefficients, since this is a low velocity region. With this definition, when the velocity decreases, the Stanton number increases, even when the heat transfer coefficient is constant. The average predicted Stanton number agrees well with the average experimental Stanton number. Comparing the Stanton number based on local velocity predictions with experimental values shows some differences in the endwall heat transfer patterns. Part of the differences in heat transfer patterns could be due to differences in the choice of ΔT used to determine the Stanton number. In the predictions the endwall pressure distribution was used to determine the local velocity for the Stanton number, as well as the adiabatic wall temperature. The reference ΔT in the experimental Stanton number was based on an experimentally determined adiabatic wall temperature. The experimental adiabatic wall temperatures were considerably lower than adiabatic wall temperatures calculated assuming a recovery factor of $Pr^{0.333}$. Using the experimentl adiabatic wall temperature to determine the predicted Stanton numbers, increases the values by up to 30%.

The third plot for the higher Mach number case shows Stanton number based on inlet velocity. Here the heat transfer coefficient and Stanton number are proportional. The maximum heat transfer occurs in the midpassage upstream of the throat. In the unguided portion of the passage there is a decrease in heat transfer across the passage in moving from the pressure side to the suction surface. This same pattern was observed by Georgiou et al.(1979) in tests of a stator vane, conducted in a shock tube facility.

Upstream of the vane the predictions show a noticeable degree of pitchwise nonuniformity. This is partially due to the interaction of the unheated starting length boundary condition with a C-type grid. C-type grids have nonuniform spacing near the mid-pitch line at the inlet, which results in pitchwise non-uniform Stanton number contours near the

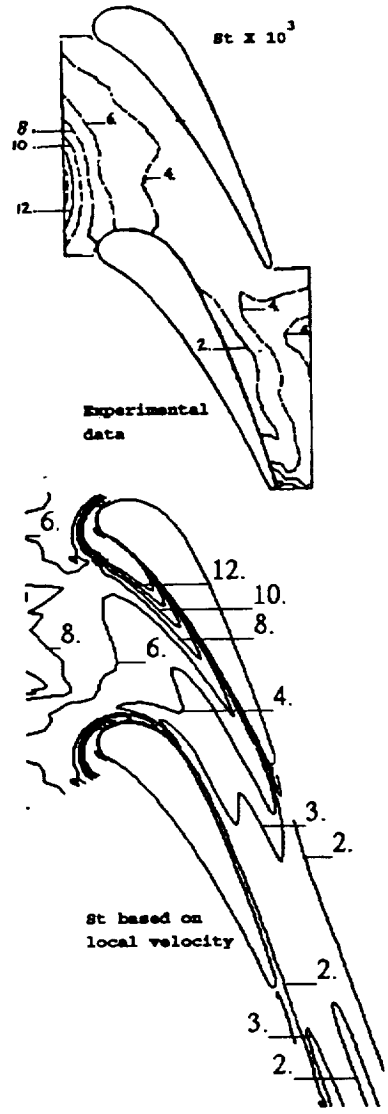

Fig. 1a - Comparison of endwall Stanton No. Data of York et al., $Re_2 = 2.1 \times 10^5, M_2 = 0.27$

endwall temperature discontinuity. However, as will be shown subsequently, C-type grids have an advantage in predicting the Stanton number in the leading edge region for the endwall and blade. Also, the Stanton number nonuniformity occurs only when there is a step change in endwall temperatures near the inlet. Calculations in which the location of the start of endwall cooling was varied, or with different grid spacing in the region on the temperature discontinuity, showed virtually identical heat transfer within the blade passage.

Although not shown in the figure, comparisons for two $M_2 = 0.70$ cases at different Reynolds numbers were very similar to the comparisons for the $M_2 = 1.1$ case shown. Considering the results for all cases, the degree of agreement between the analysis and the data is reasonably good.

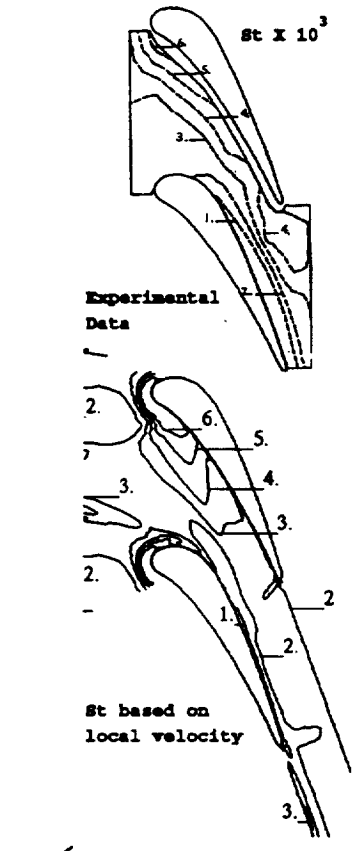

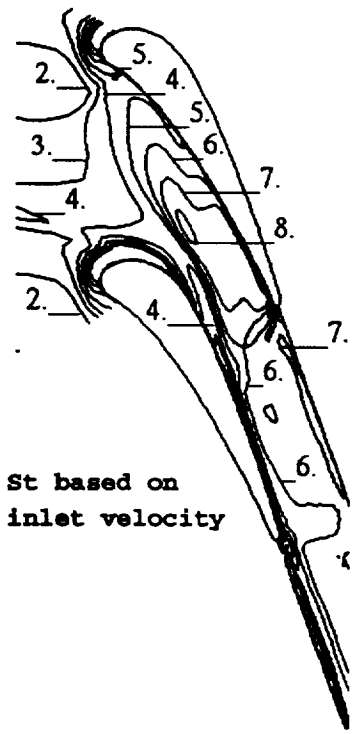

Fig. 1b - Comparison of endwall Stanton No. Data of York et al., $Re_2 = 18. \times 10^5, M_2 = 1.1$

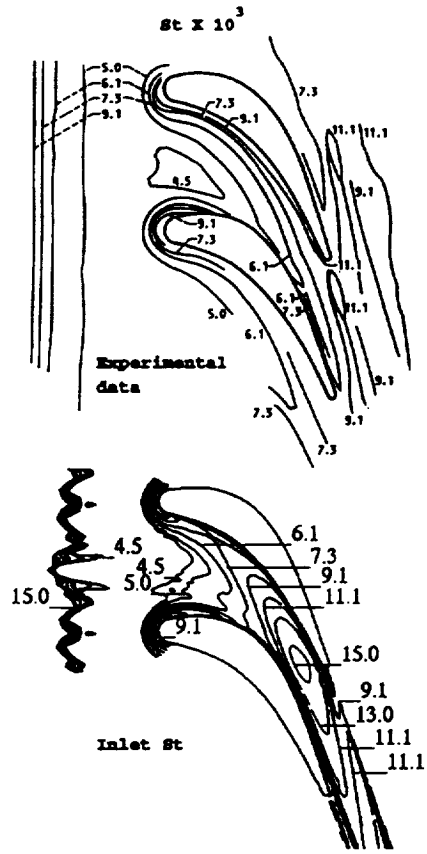

Fig. 2a - Comparison of endwall Stanton No. Data of Boyle and Russell, $Re_2 = 3.4 \times 10^5$

Data of Boyle and Russell. In these tests the Reynolds number was varied by varying the speed of the air through the cascade. Consequently, there was no independent variation of Reynolds and Mach numbers. In addition to varying the Reynolds number, the effects of variation of inlet boundary layer thickness were also presented by Boyle and Russell. The effects of variation in inlet boundary layer thickness were small. Comparisons are shown in figure 2 for a single inlet boundary layer thickness at the highest and lowest Reynolds numbers tested. Parts a and b of figure 2 compare predicted and measured Stanton numbers based on inlet conditions for two Reynolds numbers.

Within the passage the analysis overpredicts the Stanton number to a considerable extent. The region within the passage which shows the greatest disagreement is near the throat. For the low Reynolds number case the predictions show only a very small region near the pressure side of the throat with a Stanton number of 11.1×10^{-3}. But, the predictions show a peak level in excess of 15×10^{-3} in the same region. Close to the leading edge region the analysis is better agreement with the data. The liquid crystal measurements show a series of heat transfer contours in front of the leading

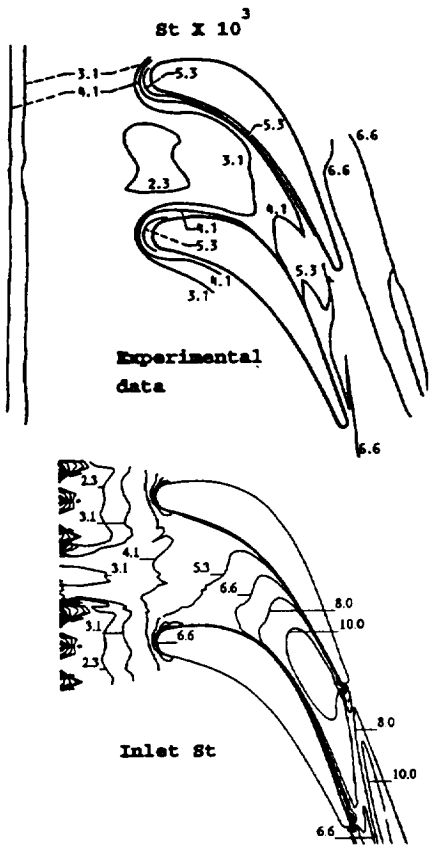

Fig. 2b - Comparison of endwall Stanton No. Data of Boyle and Russell, $Re_2 = 20 \times 10^5$

edge. The heat transfer rates increase substantially in approaching the leading edge. Boyle and Russell showed leading edge augmentation approaching a factor of three at $0.2\times$ the leading edge diameter in front of the leading edge. The predictions show a series of nearly concentric contours, which agree well with the measurements in terms of location and level of augmentation.

For the high Reynolds number case the analysis overpredicts the heat transfer in the throat region. As will be shown, a significant amount of overprediction was due to the choice of turbulence model. To insure that the discrepancy in the heat transfer prediction was due to the choice of turbulence model, other factors were examined computationally. The vane was neither heated nor cooled, and the endwall was subjected to a nearly constant heat flux. There was no significant difference in the calculated endwall heat transfer when the vane was unheated compared to when it was maintained at the endwall temperature. There was also no significant variation in endwall Stanton number when the endwall was subject to a uniform heat flux boundary condition.

Data of Arts and Heider. Figure 3 shows a comparison of the predicted and measured heat transfer data of Arts and Heider(1994). These data were obtained in a shock tube so that uncertainties due to a step change in the endwall thermal boundary condition do not arise. The data are for

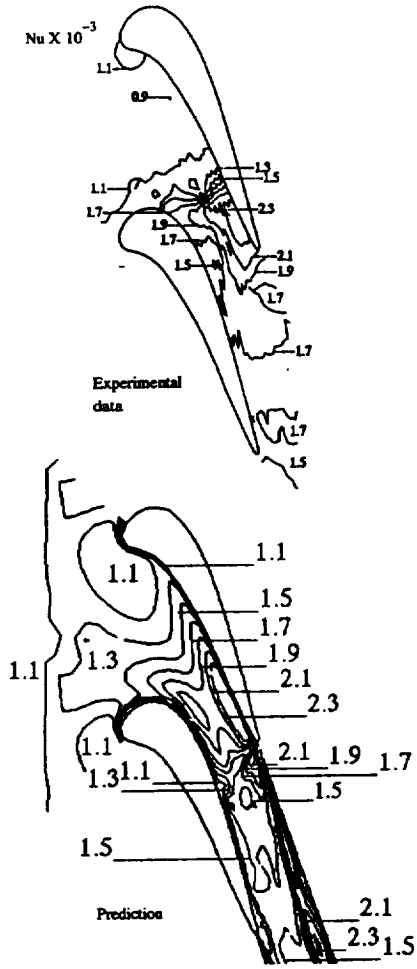

Fig. 3a- Comparison of hub Nusselt No. Data of Arts and Heider.

a stator at transonic exit conditions. The data were given as heat transfer coefficients, and have been normalized by the true chord and inlet conductivity to yield Nusselt numbers. There is good agreement between the predicted and measured Nusselt numbers for both the hub and casing surfaces.

In the experiment vane surface heat transfer measurements were made at 6%, 50%, and 94% of span. Figure 3c compares the measured and predicted heat transfer for the vane. For the pressure surface the measurements and predictions show little spanwise variation in heat transfer, though the analysis is somewhat greater than the data. Because of the high Reynolds number and moderate turbulence intensity, the predictions for the pressure surface gave transition close to the leading edge. The degree of agreement was significantly affected by the choice of transition length model. In the transition model the local turbulence intensity was adjusted based on the local freestream velocity. The analysis predicts the heat transfer well close to the endwall. At the midspan after transition, in what is essentially the uncovered portion of the vane, the analysis overpredicts the suction surface heat transfer. It will be shown that this overprediction is largely do to the choice of turbulence model.

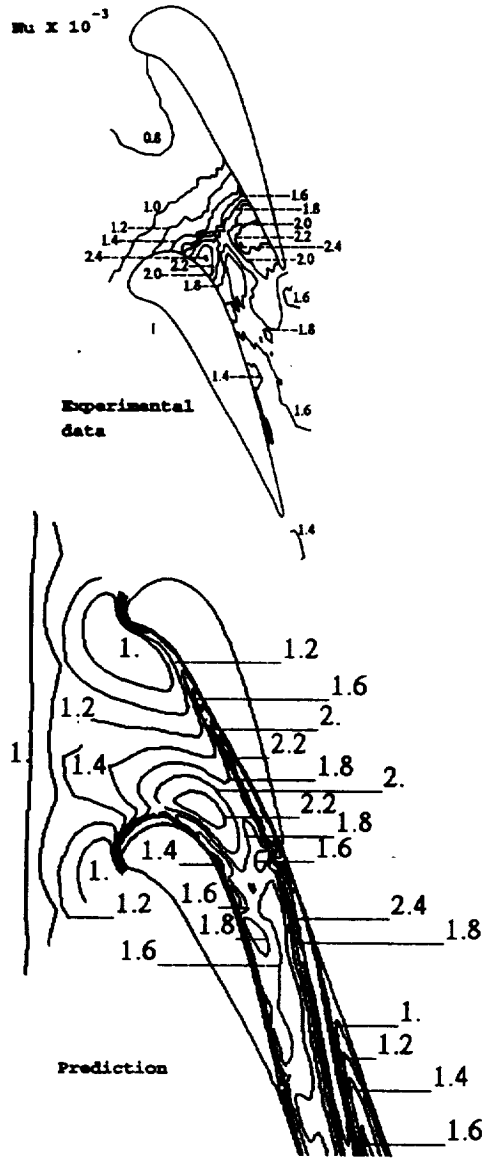

Fig. 3b Tip Nusselt No. Data of Arts and Heider.

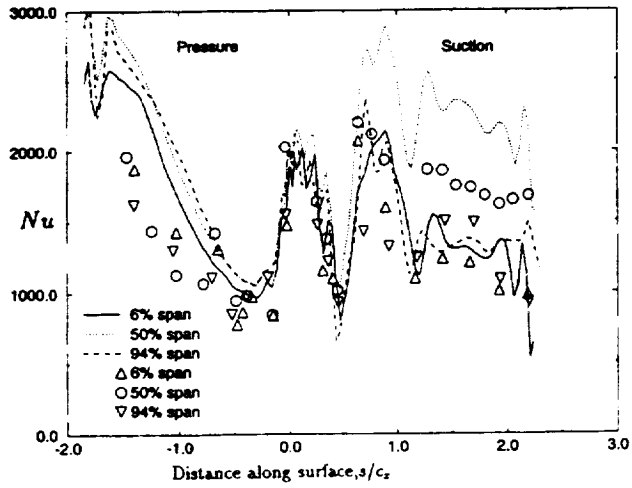

Fig. 3c Vane surface Nusselt No. Data of Arts and Heider.

Data of Harasagama and Wedlake. Figure 4 compares hub and vane heat transfer results for two different Reynolds numbers. This case is for a $M_2 = 1.14$. Vane heat transfer is mainly affected by variations in Reynolds number.

The Nusselt number varies with Reynolds number, but the degree of agreement between the prediction and measurement remains about the same. The analysis predicts a small, higher than measured, heat transfer region close to the pressure surface. Also, near the suction surface the analysis predicts a region of too low heat transfer aft of the throat region. The analysis overpredicts suction surface heat transfer in the transition region, and is slightly higher for the uncovered portion of the vane. While the variation in Nusselt number is not large, both the prediction and measurements show a lower heat transfer close to the suction surface downstream of the throat as the Mach number increases.

The degree of agreement between the analysis and the data for the casing heat transfer was about the same as for the hub. Variations in exit Mach number did not significantly affect the degree of agreement with the experimental data. The degree of agreement for the vane surface heat transfer was also not affected by variations in Mach number.

Rotors

Data of Graziani et al. Figure 5 compares the predictions with the measurements of Graziani et al. for the thin inlet boundary layer thicknesses. The measurements for the rotor surface show a slightly larger spanwise region of two-dimensional heat transfer distribution for the thinner boundary layer. In general the analysis overpredicts the heat transfer on both the rotor blade and endwall. On the rotor the analysis overpredicts the heat transfer on the rear portion of the pressure surface. This is a consequence of the transition model used. The model gave a good prediction for the suction surface transition location for the vane data of Arts and Heider. However, for this rotor case, the model predicted transition close to the leading edge. An adverse pressure gradient, close to the leading edge resulted in a calculated Re_θ sufficient to trigger transition in the turbulence model. Evidently, pressure surface transition did not occur in the experiment. On the suction surface the Stanton number is too high at transition, but otherwise the analysis predicts the heat transfer distribution reasonably well. The analysis severely overpredicts the endwall heat transfer. The largest overprediction occurs near the throat region. The effects of using a different turbulence model will be examined subsequently for this case.

Neither the measurements nor the predictions showed a large effect of varying the inlet boundary layer thickness on either the rotor blade or the endwall heat transfer. Both showed a slight decrease in peak passage heat transfer for the thicker inlet boundary layer.

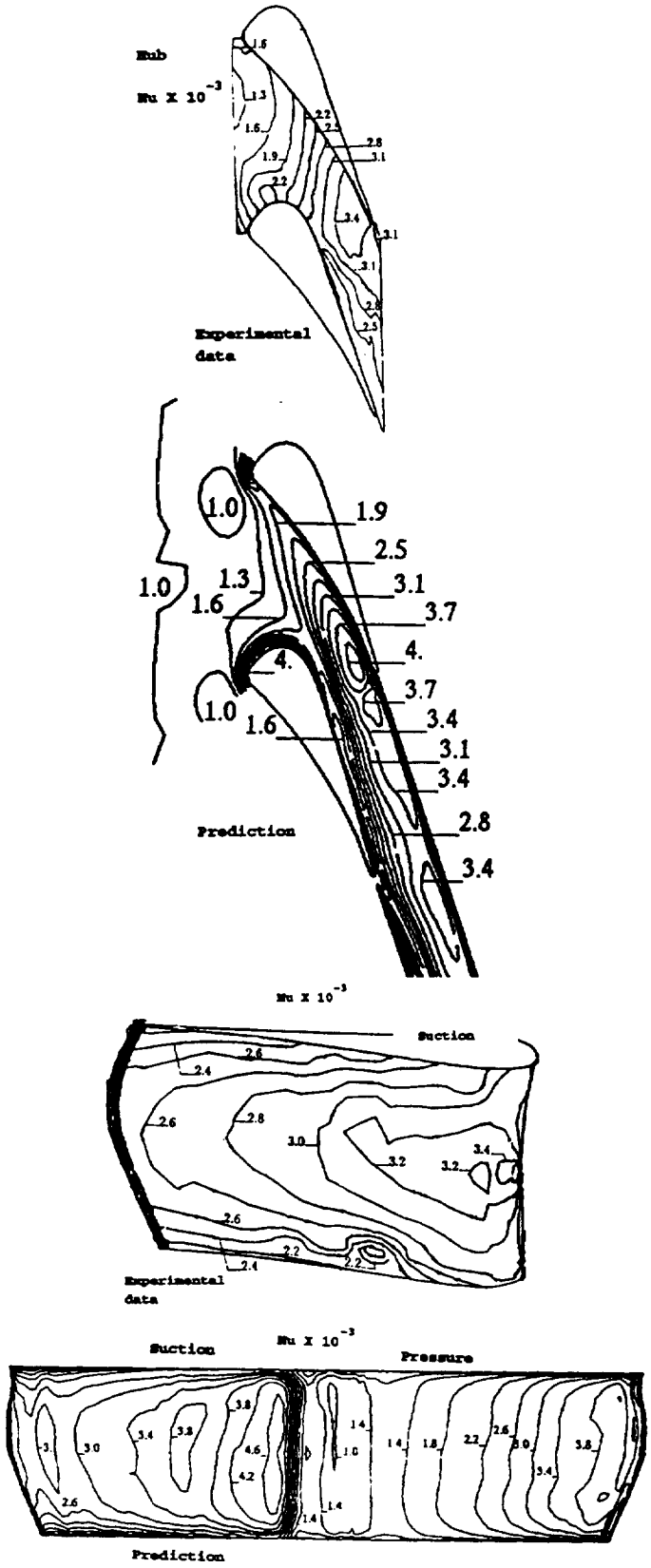

Fig. 4a- Nusselt No. comparisons. Data of Harasagama and Wedlake, $Re_2 = 34 \times 10^5, M_2 = 1.14$

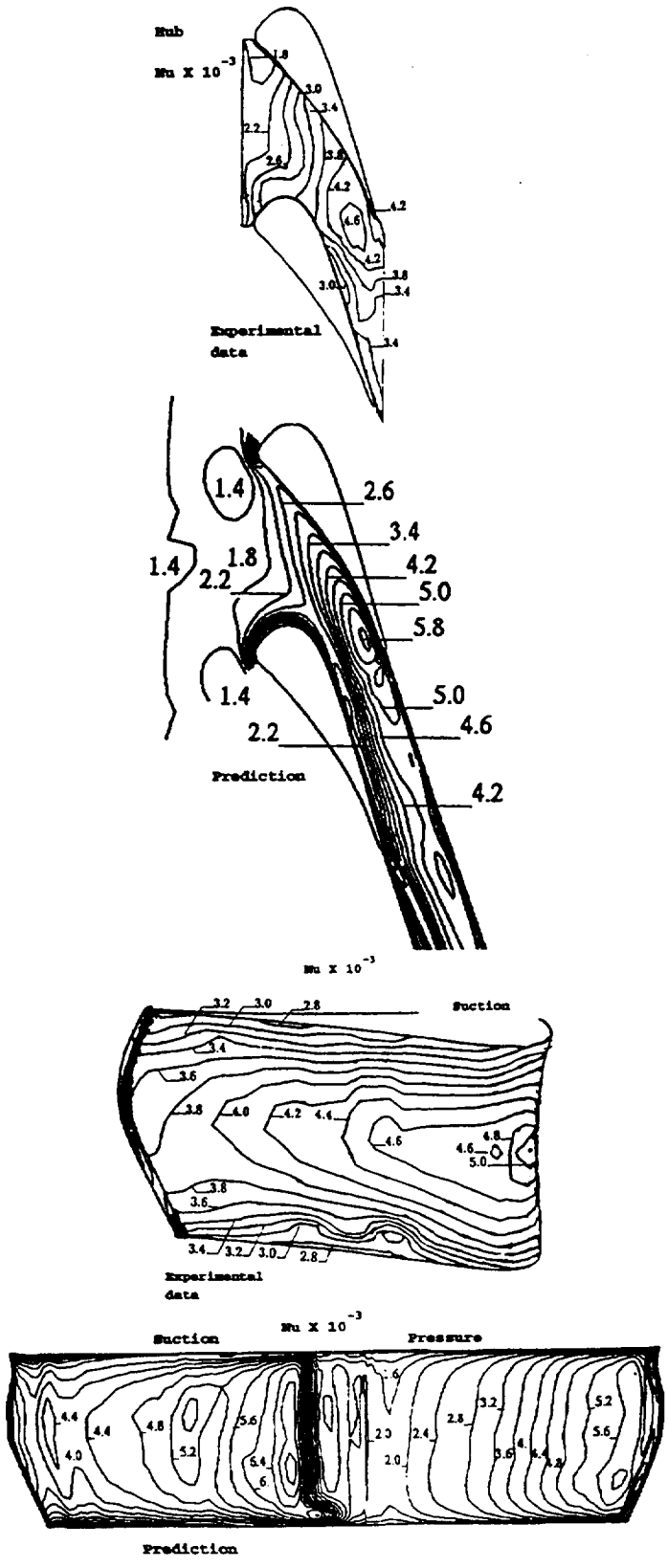

Fig. 4b- Nusselt No. comparisons. Data of Harasagama and Wedlake, $Re_2 = 54 \times 10^5, M_2 = 1.14$

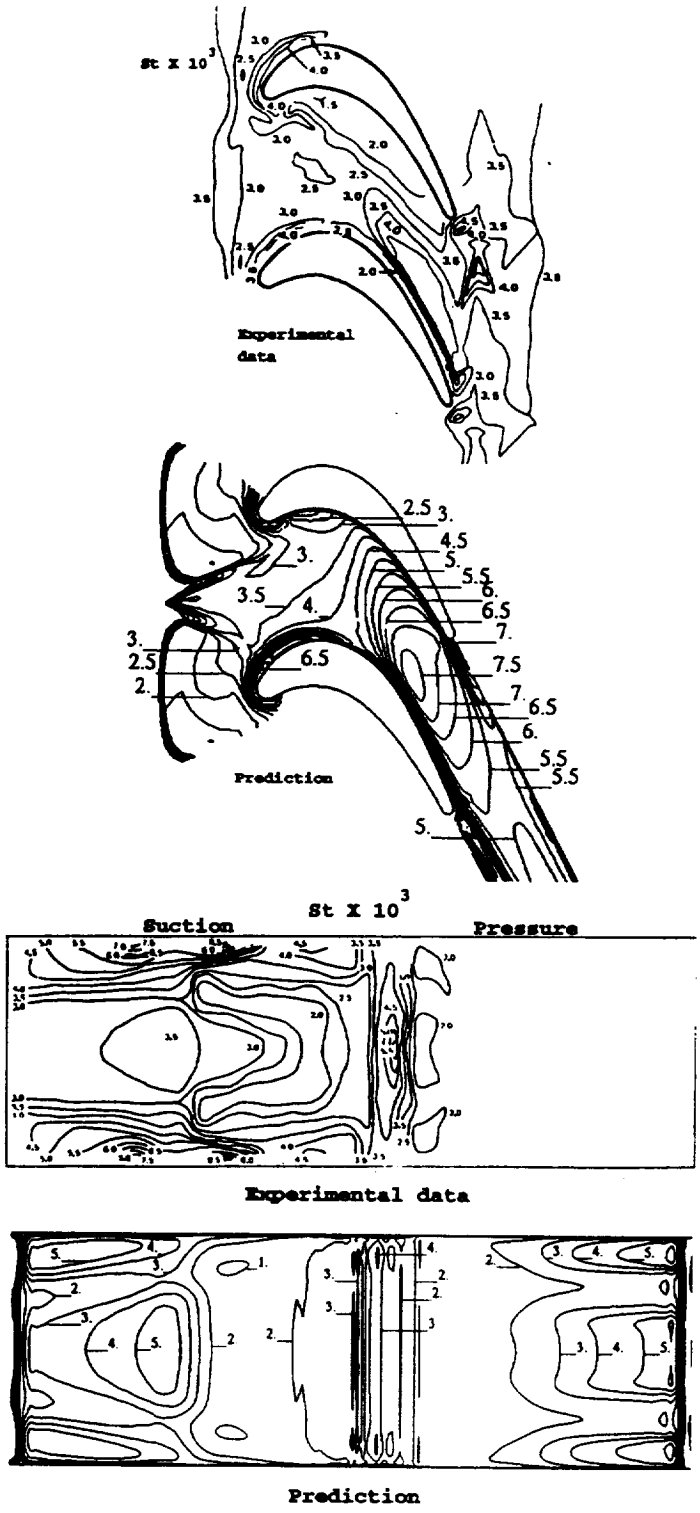

Fig. 5- Stanton No. comparisons. Data of Graziani et al.; thin inlet boundary layer.

Data of Goldstein and Spores. Figure 6a compares the predicted and measured endwall heat transfer for the higher Reynolds number-thin inlet boundary layer case of Goldstein and Spores. The data of Goldstein and Spores were normalized so that at an $x/c_x = 0.2$ upstream of the leading edge the normalized value was unity. Part of the normalization accounted for the unheated starting length. This factor was 1.24 at the point where the normalized value was unity and decreased to 1.14 at the rotor trailing edge. Predictions were normalized in the same manner. In addition to the comparison of experimental Stanton numbers, the Stanton number based on inlet conditions is shown. The nature of the napthalene measurement technique allows for very detailed localized measurements. Both the measurements and predictions show very high heat transfer in front of the leading edge, with a peak ratio in excess of 3.25. The data show the peak passage heat transfer to occur near midpassage, and somewhat upstream of the throat region. The analysis tends to overpredict the heat transfer in the throat region, but does show the correct location of the peak passage heat transfer. Comparing the two calculations shows that normalizing the Stanton number to account for the starting length has only a small effect on the shape of the endwall heat transfer distribution.

The normalized comparison does not verify the absolute level of the predicted heat transfer. Goldstein and Spores gave the mass transfer Stanton number,St_m, as 1.472×10^{-3}, where the normalized value was unity. Heat transfer predictions were converted to mass transfer values using the relationship $St = St_m(Pr/Sc)^{n-1}$. Chen and Goldstein(1992) stated that $2.0 < Sc < 2.5$, and chose $n = 0.33$. Assuming $Sc = 2.0$ yields heat transfer Stanton numbers almost exactly twice the mass transfer Stanton numbers. This ratio gives a heat transfer Stanton numbers of 0.0029, where the St_m was 1.472×10^{-3} . The predicted Stanton number at the location where the experimental Stanton number ratio was unity was 0.003. This indicates good agreement between the analysis and the experimental data in terms of the Stanton number level in the leading edge region.

There were only small differences in the experimental data among the three cases. The agreement between the predictions and the data was better for the high Reynolds number cases. Allowing the near wall damping coefficient, A^+, to be a function of the pressure gradient did not improve the agreement with the data.

Figure 6b shows comparisons for the rotor heat transfer measured by Chen and Goldstein(1992). The experimental data were presented in terms of St_m values. The predicted St values were divided by 2 for comparison purposes. There is a two-dimensional region away from the endwall, and a three-dimensional region associated with the passage vortex. The experimental suction surface data show a line separating a high heat transfer region close to the endwall from the low Stanton number region towards midspan. The predictions show the same separation into two regions, but the demarcation line does not advance up the span as rapidly, and the peak value near the endwall is lower. Also, the predictions agree with the measurements in the leading edge region. In the measurements there is a high heat transfer region towards the trailing edge, but the predictions show low values in this region. Increasing the Tu level in the analysis moved transition forward, and gave high heat transfer in this region.

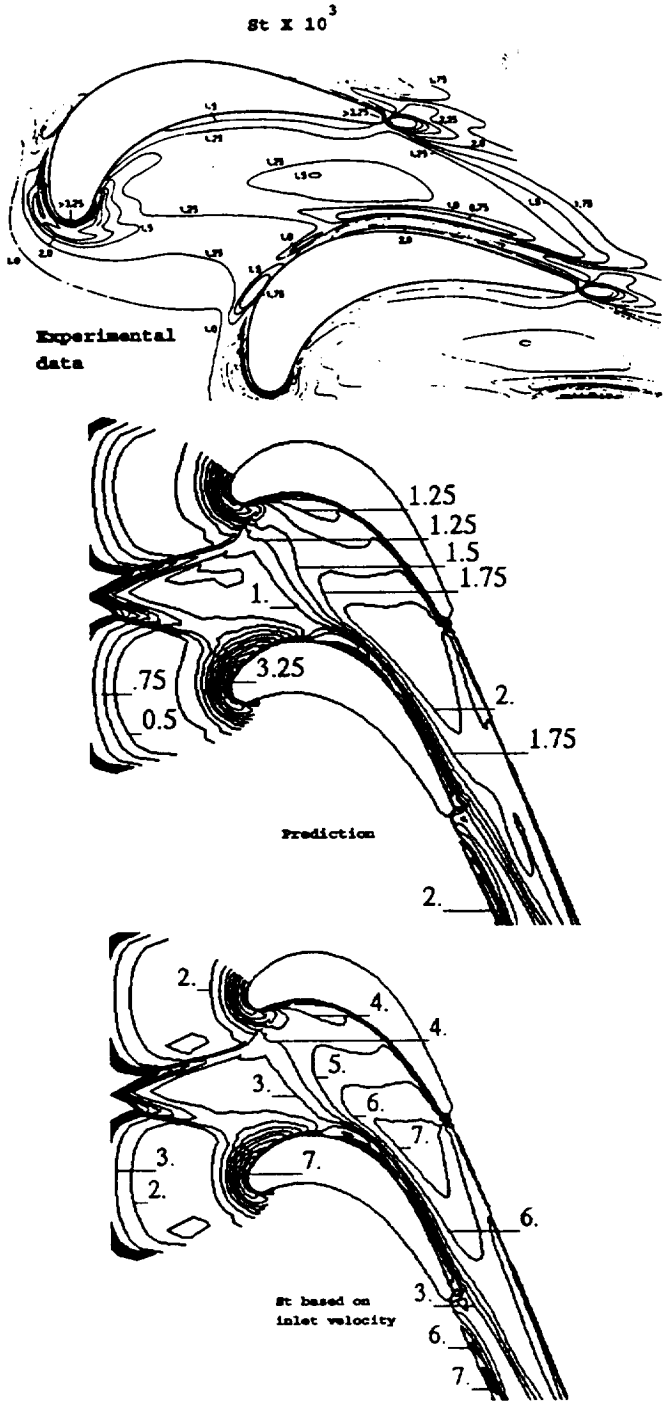

Fig. 6a - Stanton No. comparisons. Data of Goldstein and Spores, $Re_2 = 2.3 \times 10^5$, thin inlet boundary layer.

Data of Blair. Figure 7 compares predicted and measured Stanton numbers for heat transfer to the hub and blade surface for two Reynolds numbers. The Stanton numbers are based on the rotor exit relative conditions. Even though the Reynolds number varied by a factor of three, the measured Stanton numbers are only slightly lower. The predictions are only moderately lower. The expected change is not to large since assuming $St \propto Re^{-0.2}$ gives only a 25% decrease in heat transfer for a factor of three increase in Re. There is

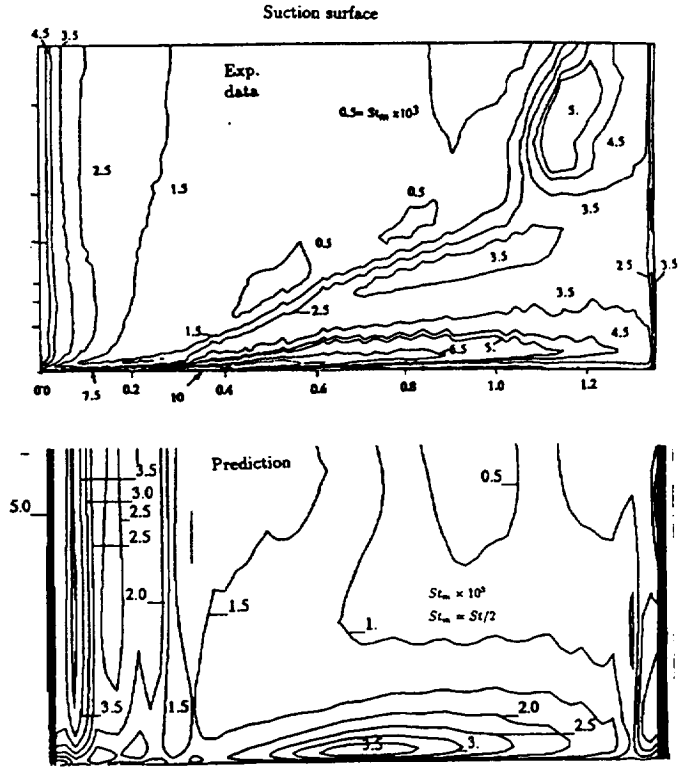

Fig. 6b - Stanton No. comparisons. Data of Chen and Goldstein.

good agreement with the data in the endwall leading edge region. The peak value predicted in the passage is somewhat greater than the experimental value, and agrees best for the high Reynolds number case. Although not shown in the measurements there is a peak predicted heat transfer level in the wake as great as the peak passage value.

The predicted rotor midspan heat transfer on the rear portion of the suction surface agrees well with the data. A Tu of 10% was used in the analysis, and resulted in transition closer to the leading edge than is evidenced by the data. The data show high heat transfer levels on the suction surface near the hub, and close to the tip, where the heat transfer is affected by the clearance flows. The analysis predicts these high heat transfer rates. In terms of the rotor hub region heat transfer, these results agree better with the data than do the predictions for the data of Chen and Goldstein(1992). The heat transfer predictions for the pressure surface are higher than the data. This is due to an early prediction for the start of transition.

Variations in the inlet flow angle did not affect the degree of agreement between the analysis and the data.

Data of Giel et al. Figure 8 compares predicted and measured Stanton numbers for two Reynolds numbers. The cases are for an $M_2 = 1.3$, and a low Tu. Predicted Stanton numbers are calculated in the same manner as the experimental

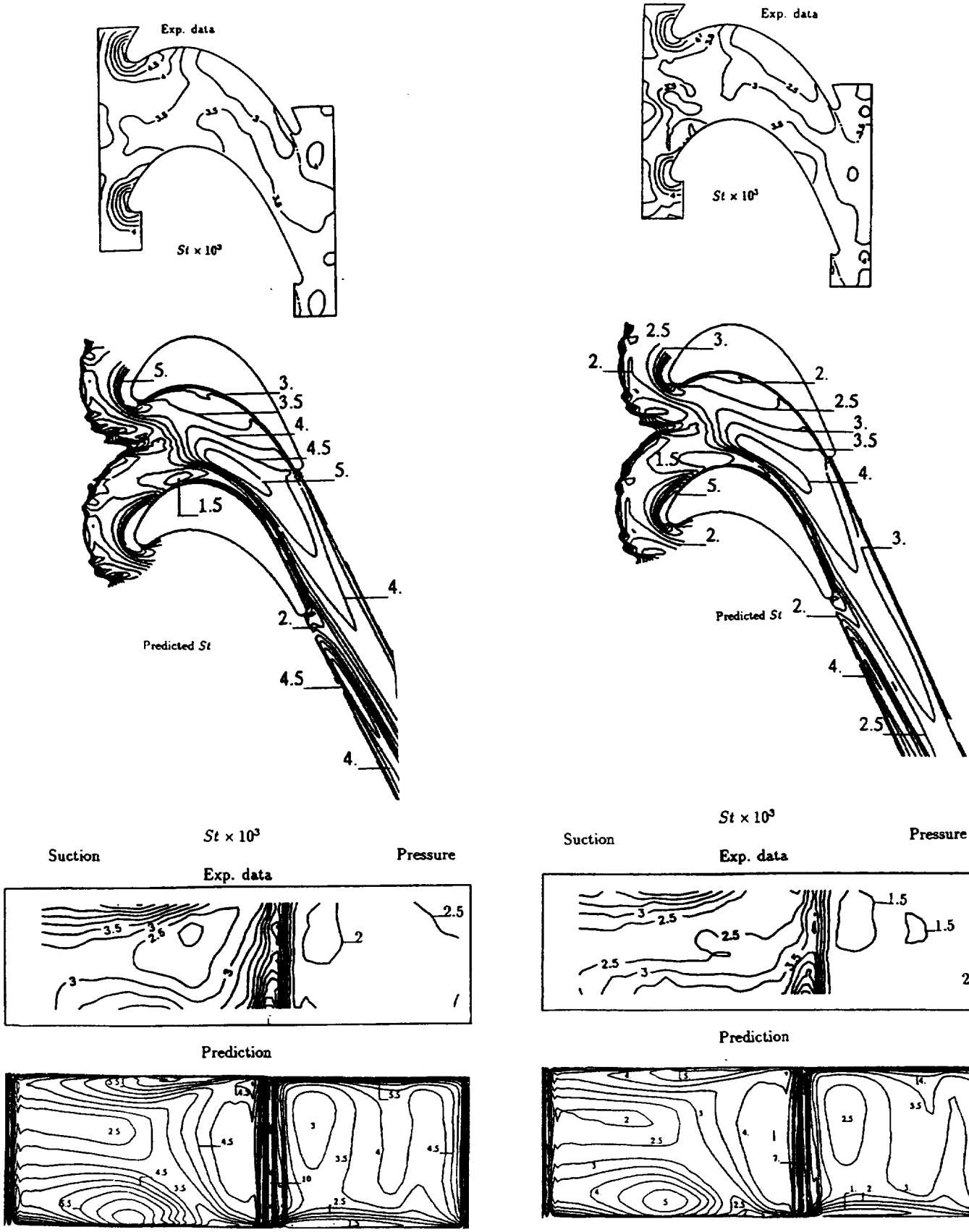

Fig. 7a- Stanton No. comparisons. Data of Blair, $Re_2 = 2.3 \times 10^5$

Fig. 7b- Stanton No. comparisons. Data of Blair, $Re_2 = 7.1 \times 10^5$

data, and is based on the calculated adiabatic wall temperature. In common with most of the previous comparisons, the agreement in the leading edge region is good. Within the passage the analysis shows a somewhat higher heat transfer level, but the correct trend in the distribution. The analysis, and especially the low Reynolds number data show what appears to be the effect of a separation line going from the pressure side leading edge region to midchord on the suction surface. In the data high heat transfer levels are seen upstream of this line, while the prediction show high levels immediately downstream of this line. Unlike several of the previous comparisons, the analysis fails to show very high heat transfer rates just downstream of the trailing edge. This may have been caused by insufficient grid resolution in this region.

Comparisons were made with the data of Giel et al. for cases in which the inlet boundary layer thickness was reduced, and in which the exit Mach number was reduced to 1.0. The reduced inlet boundary layer thickness resulted in reduced secondary flows. The measured endwall heat transfer near the pressure surface just upstream of the throat was lowered when there was a thinner inlet boundary layer. The analysis showed the same behavior. Reducing the exit Mach number gave slightly higher heat transfer downstream of the throat. This effect was also seen in the predictions.

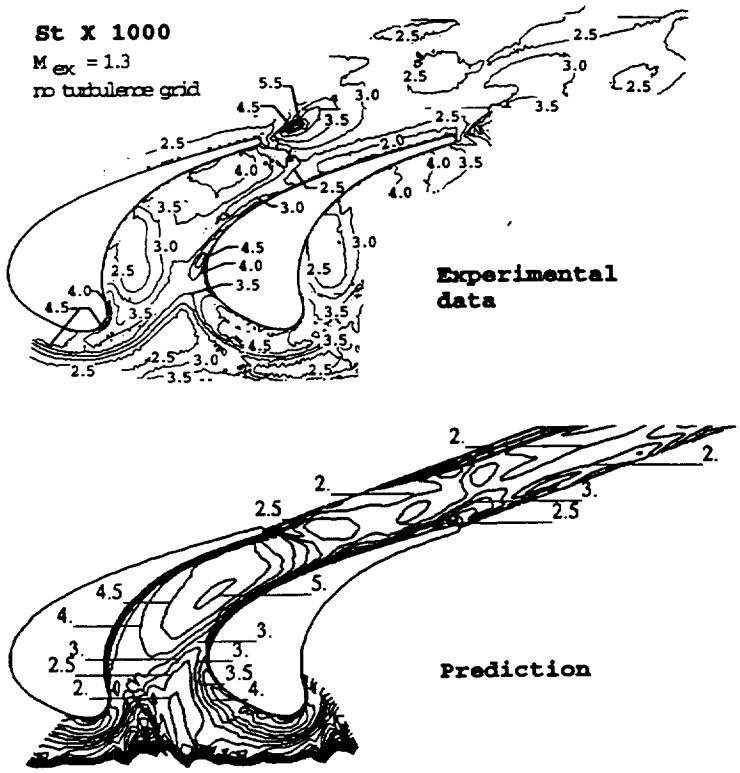

Fig. 8a. Stanton No. comparisons, Data of Giel et al., $Re_2 = 26 \times 10^5, M_2 = 1.3$

Turbulence model effects

All of the comparisons shown so far have been for the turbulence model described by Chima et al.(1993). The comparisons that were given showed the predicted heat transfer was generally higher than the measurements. For comparisons where T_w/T_g' was characteristic of engine operating conditions, the degree of overprediction was small. For comparisons where T_w/T_g' was small, and the Mach number was low, the degree of overprediction was high. The primary cause of these results is the choice of turbulence model. Results presented in this section illustrate the effects of an alternative algebraic turbulence model on heat transfer predictions. These comparisons illustrate the sensitivity of the heat transfer predictions to the choice of turbulence model. The predictions shown in this section were obtained using the Baldwin-Lomax(1978) turbulence model. Predictions shown using this model will be labeled as Baldwin-Lomax results. The following figures illustrate the differences in heat transfer attributable solely to differences in the turbulence models.

Figure 9 shows the prediction using the Baldwin-Lomax turbulence model for the same test case as in figure 2b. The Stanton numbers are in better agreement with the data using the Baldwin-Lomax model. The peak endwall heat transfer has been reduced considerably, and is in closer agreement with the experimental data.

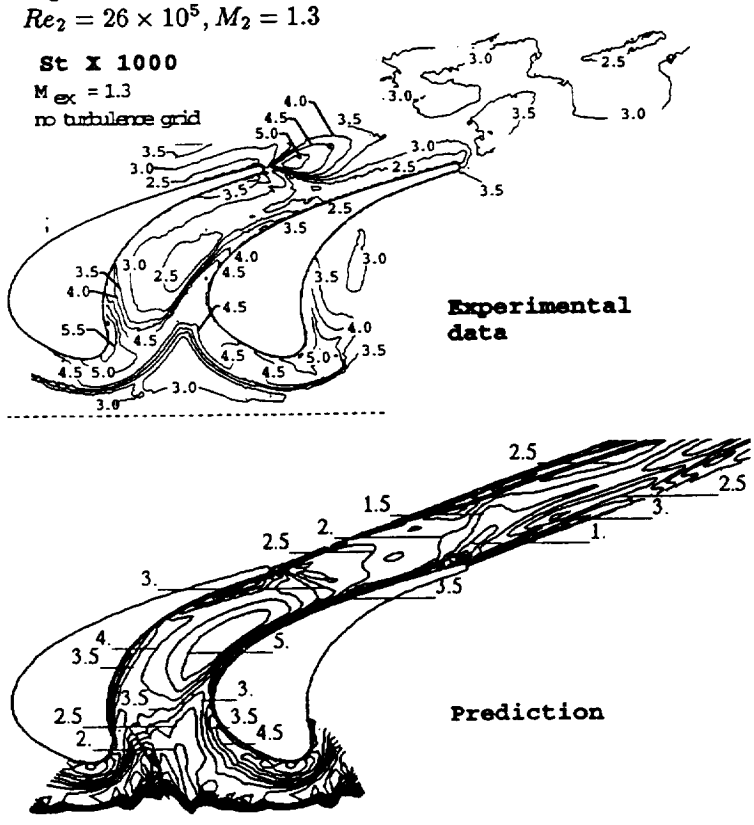

Fig. 8b. Stanton No. comparisons, Data of Giel et al., $Re_2 = 13 \times 10^5, M_2 = 1.3$

Figure 10 shows prediction using the Baldwin-Lomax model for the test case in figure 3. Only the hub endwall prediction is shown. The relative differences between the two predictions were the same for the hub and tip. The vane surface prediction in figure 10 shows better agreement with the presssure and suction surface data than the comparison shown in figure 3c. There are differences in the vane suction surface heat transfer between the two predictions. The predictions in figure 10 were calculated assuming the turbulence intensity remained constant. This caused the start of transition to move forward on the suction surface. The data indicate that the assumption of variable turbulence intensity gives better agreement for the transition location. The hub heat transfer prediction using the Baldwin-Lomax model does not agree with the experimental results better than the prediction using Chima's turbulence model. The predictions using the Baldwin-Lomax model are significantly lower near the vane suction surface beyond the throat.

Figure 11 shows the prediction for design condition used by Harasagama and Wedlake(1991). These results should be compared with the data in figure 4a. The effect of varying the turbulence Model for this test case are very similar to the results shown in the previous figure for the data of Arts and Heider. The vane surface heat transfer prediction is somewhat improved, but the endwall heat transfer prediction agrees less well with the experimental data.

There is a high degree of similarity between the predictions for the data of Goldstein and Spores, and for the data of Graziani et al.(1980). The effects of varying the turbulence model were the same for the two configurations. Figure 12 shows the hub and rotor surface predictions for the same case as given in figure 5. Somewhat surprisingly, substituting the Baldwin-Lomax turbulence model has only a small effect on the endwall heat transfer. The predicted heat transfer is still significantly higher than the data. The results shown in figure 12 for the vane surface illustrate two independent effects. For the suction surface the figure illustrates the effect of a different turbulence model. The effects are small. For the pressure surface figure 12 illustrates the effect of suppressing transition. A laminar calculation for the pressure surface is in good agreement with the experimental data.

Using the Baldwin-Lomax turbulence model to predicted the high Reynolds number rotor test case of Blair(1994) is illustrated in figure 13. These results should be compared with those shown in figure 7b. Here the effect of varying the turbulence model is relatively small. The flow distribution determined for a rotating blade with clearance appears to have the dominant effect on surface heat transfer.

Figure 14 illustrates the effect of using the Baldwin-Lomax turbulence model for the high Reynolds number test case of Giel et al. These predictions should be compared with the results in figure 8a. These heat transfer rates are lower than those calculated using Chima's turbulence model. Chima's model gives heat transfer rates that are in better agreement with the experimental data.

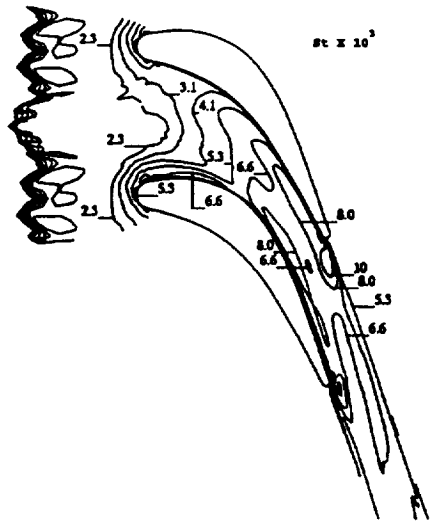

Fig. 9. Prediction of high Reynolds number case of Boyle and Russell with Baldwin-Lomax turbulence model.

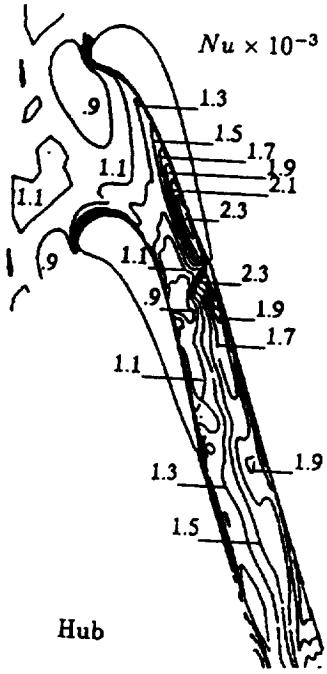

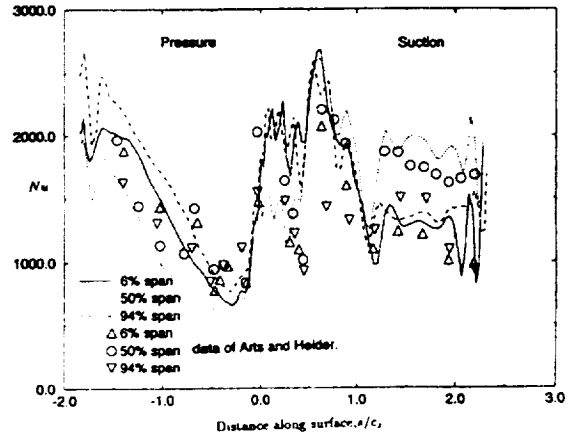

Fig. 10. Prediction of Arts and Heider case with Baldwin-Lomax turbulence model.

Both Chima's turbulence model and the Baldwin-Lomax model are two layer models, and have the same inner layer formulation. The outer layer eddy viscosity is determined differently in each model. These differences, which are described by Chima et al.(1993), give rise to the differences in the heat transfer predictions. Greater outer layer eddy viscosities are associated with higher heat transfer rates. Increased outer layer eddy viscosities result from increased wall distances at which the outer layer values are determined.

CONCLUDING REMARKS

Comparisons were shown between predicted and measured blade and endwall heat transfer for data obtained from a variety of sources. Unfortunately, one turbulence model did not give good agreement for all cases. For all of the cases examined the baseline model gave peak heat transfer rates as high or higher than the measured values. Those cases for which the wall-to-gas temperature ratio was characteristic of actual engine conditions had predicted heat transfer rates in good agreement with the data overall. The predictions were only slightly higher on the endwall at the peak location in the throat region. Overall, the model was conservative in that it gave higher than measured heat transfer rates.

Comparisons for cases with wall-to-gas temperature ratios not typical of actual engine operation, and low Mach numbers showed that the baseline turbulence model was conservative, perhaps to an unacceptably high degree. An alternate turbulence model gave reasonably good heat transfer predictions for these test cases. However, this model underpredicted the heat transfer for cases with wall-to-gas temperature ratios representative of actual engine operation.

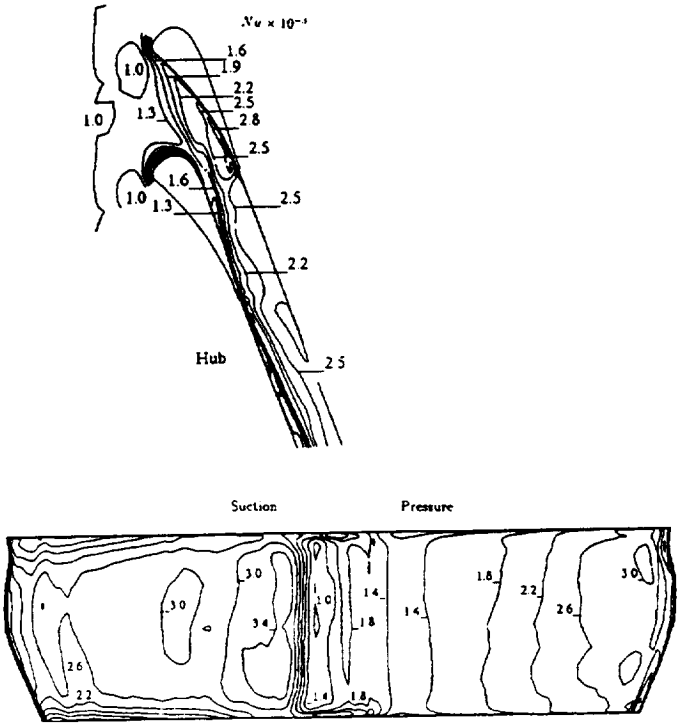

Fig. 11 Prediction of high *Re* case of Harasagama and Wedlake with Baldwin-Lomax turbulence model.

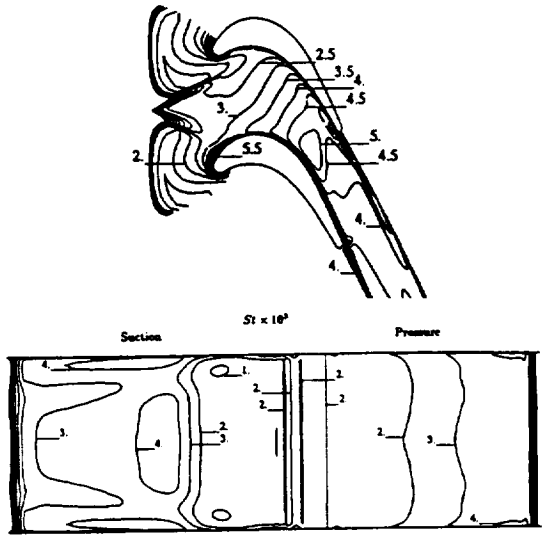

Fig. 12. Prediction of Graziani et al. with Baldwin-Lomax turbulence model.

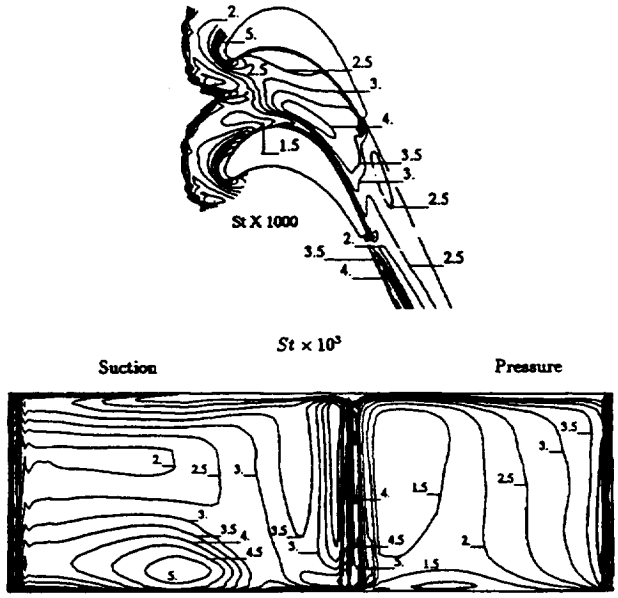

Fig. 13. Prediction of Blair's high *Re* case with Baldwin-Lomax turbulence model.

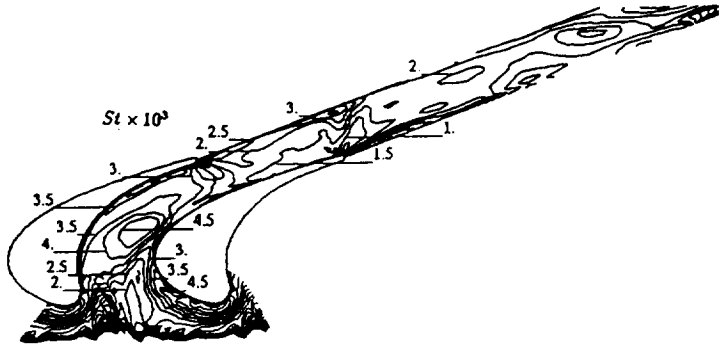

Fig. 14 Prediction of high Reynolds number case of Giel et al. with Baldwin-Lomax turbulence model.

REFERENCES

Ameri, A.A. and Arnone, A., 1994, "Prediction of Turbine Blade Passage Heat Transfer Using a Zero and a Two-Equation Turbulent Model," ASME Paper 94-GT-122.

Arnone, A, Liou, M.-S, and Povinelli, L. A., 1992, "Navier-Stokes Solution of Transonic Cascade Flows Using Non-Periodic C-Type Grids," AIAA *Journal of Propulsion and Power*, Vol. 8, No.2, pp 410-417.

Arts, T, and Heider, R., 1994, "Aerodynamic and Thermal Performance of a Three Dimensional Annular Transonic Nozzle Guide Vane. Part I: Experimental Investigation," AIAA Paper AIAA-94-2929.

Baldwin, B.S. and Lomax, H., 1978, "Thin- Layer Approximation and Algebraic Model for Separated Turbulent Flows," AIAA Paper AIAA-78-257.

Blair, M. F., 1974, "An Experimental Study of Heat Transfer and Film Cooling in Large-Scale Turbine Endwalls," ASME *Journal of Heat Transfer*, Vol 96, pp.525-529, 1974.

Blair, M. F., 1994, "An Experimental Study of Heat Transfer in a Large-Scale Turbine Rotor Passage," ASME *Journal of Turbomachinery*, Vol. 116, No. 1, pp 1-13.

Boyle, R. J, and Russell, L. M., 1990, "An Experimental Determination of Stator Endwall Heat Transfer," ASME *Journal of Turbomachinery*, Vol 112, pp.547-558.

Boyle, R. J, and Jackson, R., 1995,"Heat Transfer Predictions for Two Turbine Nozzle Geometries at High Reynolds and Mach Numbers," ASME paper 95-GT-104.

Boyle, R.J., and Giel, P.W., 1992, "Three-Dimensional Navier-Stokes Heat Transfer Predictions for Turbine Blade Rows," AIAA paper AIAA-92-3068.

Boyle, R.J., and Ameri, A., 1994, "Grid Orthogonality Effects onPredicted Turbine Midspan Heat Transfer and Performance," ASME paper 94-GT-123.

Cebeci, T., and Smith, A.M.O., 1974, "*Analysis of Turbulent Boundary Layers*, Acedemic Press, New York.

Chen, P.H., and Goldstein, R. J., 1992, "Convective Transport Phenomena on the Suction Surface of a Turbine Blade Including the Influence of Secondary Flows Near the Endwall," ASME *Journal of Turbomachinery*, Vol 114, No. 4, pp.776-787.

Chana, K.S., 1992, "Heat Transfer and Aerodynamics of a High Rim Speed Turbine Nozzle Guide Vane with Profiles End Walls," ASME paper 92-GT-243.

Chima, R.V., and Yokota, J.W., 1988, "Numerical Analysis of Three-Dimensional Viscous Internal Flows," AIAA paper 88-3522, (NASA TM-100878).

Chima, R.V., 1991, "Viscous Three-Dimensional Calculations of Transonic Fan Performance," AGARD Propulsion and Energetics Symposium on Computational Fluid Mechanics for Propulsion, San Antonio, Texas, May 27-31.

Chima, R.V., Giel, P.W., and Boyle, R.J., 1993, "An Algebraic Turbulence Model for Three-Dimensional Viscous Flows," AAIA paper 93-0083, (NASA TM-105931).

Choi, D., and Knight, C.J., 1988, "Computations of 3D Viscous Linear Cascade Flows," AIAA *Journal* Vol. 26, No. 12, pp 1477-1482.

Georgiou, D. P., Godard, M., and Richards, B. E., 1979, "Experimental Study of the Iso-Heat-Transfer-Rate Lines on the End-Wall of a Turbine Cascade," ASME paper 79-GT-20.

Giel, P.W., Thurman, D.R., Van Fossen, G.J., Hippensteele, S.A., and Boyle, R.J., 1996, "Endwall Heat Transfer Measurements in a Transonic Turbine Cascade," To be presented at the ASME Gas Turbine Conference, June 10-13, Birmingham, UK.

Goldstein, R.J., and Spores, R.A., 1988 "Turbulent Transport on the Endwall in the Region Between Adjacent Turbine Blades", ASME *Journal of Heat Transfer*, Vol. 110, No. 4, pp 862-869.

Graziani, R.A., Blair, M.F., Taylor, R.J., and Mayle, R.E., 1980, "An Experimental Study of Endwall and Airfoil Surface Heat Transfer in a Large Scale Turbine Blade Cascade," *Journal of Engineering for Power*, Vol. 102, No. 2, pp. 1-11.

Hah, C., 1989,"Numerical Study of Three-Diensional Flow and Heat Transfer Near the Endwall of a Turbine Blade Row," AIAA paper 89-1689.

Harasagama, S.P., Wedlake, E.T., 1991, "Heat Transfer and Aerodynamics of a High Rim Speed Turbine Nozzle Guide Vane Tested in the RAE Isentropic Light Piston Cascade(ILPC)," ASME *Journal of Turbomachinery*, Vol. 113, No. 4, pp 384-391.

Heider, R. and Arts, T., 1994, "Aerodynamic and Thermal Performance of a Three Dimensional Annular Transonic Nozzle Guide Vane. Part II: Assessment of a 3D Navier-Stokes Solver," AIAA Paper AIAA-94-2930.

Hylton, L. D., Mihelc, M. S., Turner, E. R., York, R. E., 1981, "Experimental Investigation of Turbine Endwall Heat Transfer," Detroit Diesel Allison Report EDR 10363, Volumes I-III, (Aero Propulsion Laboratory Report AFWAL-TR-81-2077, Volumes I-III.)

Kays, W.M., Crawford, M.E., *Convective Heat and Mass Transfer*, McGraw-Hill Pub. Co., 1980.

Mayle, R.E., 1991, "The role of Laminar-Turbulent Transition in Gas Turbine Engines," ASME *Journal of Turbomachinery*, Vol. 113, pp 509-537.

Smith, M.C., and Kuethe, A.M., 1966, "Effects of Turbulence on Laminar Skin Friction and Heat Transfer," Physics of Fluids, Vol. 9, pp. 2337-2344.

Sorenson, R.L., 1980, "A Computer Program to Generate Two-Dimensional Grids About Airfoils and Other Shapes by the Use of Poisson's Equation,", NASA TM 81198.

York, R. E., Hylton, L.D., and Mihelc, M. S., 1984, "Experimental Endwall Heat Transfer and Aerodynamics in a Linear Vane Cascade," ASME *Journal of Engineering for Gas Turbines and Power*, Vol 106, pp.159-167.

REPORT DOCUMENTATION PAGE

Form Approved
OMB No. 0704-0188

1. AGENCY USE ONLY (*Leave blank*)	2. REPORT DATE	3. REPORT TYPE AND DATES COVERED
	November 1996	Technical Memorandum

4. TITLE AND SUBTITLE

Predicted Turbine Heat Transfer for a Range of Test Conditions

5. FUNDING NUMBERS

WU-505-62-52

6. AUTHOR(S)

R.J. Boyle and B.L. Lucci

7. PERFORMING ORGANIZATION NAME(S) AND ADDRESS(ES)

National Aeronautics and Space Administration
Lewis Research Center
Cleveland, Ohio 44135-3191

8. PERFORMING ORGANIZATION REPORT NUMBER

E-10543

9. SPONSORING/MONITORING AGENCY NAME(S) AND ADDRESS(ES)

National Aeronautics and Space Administration
Washington, D.C. 20546-0001

10. SPONSORING/MONITORING AGENCY REPORT NUMBER

NASA TM-107374

11. SUPPLEMENTARY NOTES

Prepared for the 41st Gas Turbine and Aeroengine Congress sponsored by the International Gas Turbine Institute of the American Society of Mechanical Engineers, Birmingham, United Kingdom, June 10-13, 1996. Responsible person, R.J. Boyle, organization code 2640, (216) 433-5889.

12a. DISTRIBUTION/AVAILABILITY STATEMENT

Unclassified - Unlimited
Subject Category 34

This publication is available from the NASA Center for AeroSpace Information, (301) 621-0390.

12b. DISTRIBUTION CODE

13. ABSTRACT (*Maximum 200 words*)

Comparisons are shown between predictions and experimental data for blade and endwall heat transfer. The comparisons are given for both vane and rotor geometries over an extensive range of Reynolds and Mach numbers. Comparisons are made with experimental data from a variety of sources. A number of turbulence models are available for predicting blade surface heat transfer, as well as aerodynamic performance. The results of an investigation to determine the turbulence model which gives the best agreement with experimental data over a wide range of test conditions are presented.

14. SUBJECT TERMS

Turbine; Heat transfer; Navier-Stokes

15. NUMBER OF PAGES

18

16. PRICE CODE

A03

17. SECURITY CLASSIFICATION OF REPORT	18. SECURITY CLASSIFICATION OF THIS PAGE	19. SECURITY CLASSIFICATION OF ABSTRACT	20. LIMITATION OF ABSTRACT
Unclassified	Unclassified	Unclassified	